EVALUATION OF A FUZZY LOGIC BASED COMPUTER AIDED DIAGNOSIS SYSTEM FOR CHEST X-RAY NODULE DETECTION AND CHARACTERIZATION

by

Nurhan Öztürk

B.Sc., Biomedical Engineering, Başkent University, 2012

Submitted to the Institute of Biomedical Engineering

in partial fulfillment of the requirements

for the degree of

Master of Science

in

Biomedical Engineering

Boğaziçi University

2015

EVALUATION OF A FUZZY LOGIC BASED COMPUTER AIDED DIAGNOSIS SYSTEM FOR CHEST X-RAY NODULE DETECTION AND CHARACTERIZATION

APPROVED BY:

Assoc. Prof. Dr. Albert Güveniş   . . . .

(Thesis Advisor)

Assist. Prof. Dr. Bora Garipcan   . . . .

Assoc. Prof. Dr. Mehmet Burçin Ünlü   . . . .

DATE OF APPROVAL: 31 July 2015

ACKNOWLEDGMENTS

I would like to express my sincere gratitude to my advisor Assoc. Prof. Dr. Albert Güveniş for his kindness and valuable advices, suggestions, feedback and encouragement during the research.

I also want to thank my friends at the institute for their company.

My special gratitude goes to the best dorm mates Melike Hendek and Zehra Gökpınar for the time spent together. Their support and company mean so much to me.

I specially thank my dear friends Melis Kaygusuz, Gizem Birman and Olgu Benli for their motivation. Life in Istanbul would be harder without their support.

I also want to thank Dr. Ülkühan Güler and Arslan Güler for being my second family in Istanbul.

Finally, I would like to thank my dear family for their encouragement, guidance and love throughout my life. I am proud of being your daughter.

ABSTRACT

EVALUATION OF A FUZZY LOGIC BASED COMPUTER AIDED DIAGNOSIS SYSTEM FOR CHEST X-RAY NODULE DETECTION AND CHARACTERIZATION

Computer aided systems has a crucial importance on lung nodule studies, since lung cancer is the leading cause of cancer related death for both men and women worldwide. Accurate characterization of lung nodules as malignant or benign may be difficult. CAD can assist radiologists in improving the accuracy of classification. The computer-assisted characterization of lung nodules involves several steps including segmentation, feature extraction and classification. In this study, we aim to optimize each step in order to improve the overall accuracy through on classification accuracy. The main objective of this study is to improve the characterization of detected nodules on chest x-rays by performance comparison of algorithms and optimum selection of classifier parameters. In this study, 154 posteroanterior chest x-ray images included in JSRT Database were used as test materials. The database consists of 100 malignant and 54 benign nodules. Our system involves pre-processing, detection, segmentation, feature extraction and classification steps. The aim of the pre-processing was to improve the quality of the images by contrast enhancement and noise reduction. We have determined 14 features (morphological features, statistical features and textural features) from each segmented nodule to make the classification more efficient. Initially in this work we have used k-nearest neighbor classifier and fuzzy classifier to classify the nodules as malignant or benign. We have tested the algorithm for different parameter values. According to our initial results, the optimal accuracy for k-NN classification is 68.8% and for the fuzzy classification it is 61.3%. The initial results reveal that this methodology has the potential to assist radiologists as a second opinion tool in the classification of benign and malignant lung nodules.

Keywords: CAD,Chest X-ray, Lung Nodule Characterization, Fuzzy Classification.

ÖZET

AKCİĞER GRAFİSİNDE NODÜLLERİN BELİRLENMESİNDE ve SINIFLANDIRILMASINDA BULANIK MANTIĞA DAYALI BİLGİSAYAR DESTEKLİ TANI SİSTEMİNİN DEĞERLENDİRİLMESİ

Akciğer kanseri, dünyada hem kadınlar hem de erkekler için kanser ölümlerinin başında geldiği için akciğer kanserleri üzerindeki bilgisayar destekli çalışmalar büyük bir öneme sahiptir. Akciğer nodüllerinin kanserli ve kansersiz olarak kesin ayrımını yapmak zor olabilmektedir. Bilgisayar destekli tanı sistemleri bu ayrımı yapmak konusunda radyologlara yardımcı olmaktadır. Akciğer nodüllerinin bilgisayar destekli ayrımı; bölme, özellik belirleme ve sınıflandırma gibi çeşitli aşamalardan oluşmaktadır. Bu çalışmada, her bir aşamayı optimize ederek sınıflandırma doğruluğunu geliştirmeyi amaçlamaktayız.Bu çalışmanın temel amacı, algoritmaların performans kıyaslamasını yaparak ve en uygun sınıflandırma parametrelerini seçerek, x-ray görüntüleri üzerinde belirlenmiş nodüllerinin tanımlama oranını arttırmaktır. Bu çalışmada, JSRT veri tabanında bulunan 154 tane önden çekilmiş x-ray göğüs görüntüsü test materyali olarak kullanılmıştır. Veritabanı 100 tane kanserli ve 54 tane kansersiz nodül içermektedir. Bizim sistemimiz; ön işlem, belirme, ayırma, özellik belirleme ve sınıflandırma aşamalarından oluşmaktadır. Ön işlemin amacı kontrast iyileştirme ve gürültü azaltımı uygulanarak, görüntülerin kalitesini arttırmaktır. Sınıflandırmayı daha verimli hale getirmek için ayrılmış nodüllerden 14 tane özellik (biçimsel özellikler, istatistiksel özellikler ve dokusal özellikler) belirledik. Bu çalışmada nodülleri kanserli ve kansersiz olarak ayırmak için öncelikle, en yakın komşuluk yöntemi ve bulanık mantık yöntemi kullanılmıştır. Sistemi farklı parametre değerleri için test ettik. Elde ettiğimiz ilk sonuçlara göre, optimum doğruluk değeri en yakın komşuluk yöntemine göre %68.8 ve bulanık mantık yöntemine göre %61.3'tür. Elde ettiğimiz ilk sonuçlar bu yöntemin radyologların akciğer nodüllerini kanserli ve kansersiz olarak ayırmasında ikinci bir fikir sunma amacıyla kullanılabileceğini göstermiştir.

Anahtar Sözcükler:CAD, X-ray, Akciğer Nodül Nitelendirme, Bulanık Sınıflandırma.

TABLE OF CONTENTS

LIST OF FIGURES

LIST OF TABLES

LIST OF ABBREVIATIONS

CAD	Computer Aided Diagnosis
CT	Computed Tomography
MRI	Magnetic Resonance Imaging
PET	Positron Emission Tomography
KNN	K Nearest Neigbor
PA	Posteroanterior
ANN	Artificial Neural Network
LDA	Linear Discriminant Analysis
JSRT	Japanese Society of Radiological Technology
LOOCV	Leave One Out Cross Validation

1. INTRODUCTION

Lung cancer is one of the most common cancers in the world. Majority of cancer deaths are from lung cancer [1]. Medical imaging has a crucial impact on the early detection of cancer. In case of lung cancer, imaging technologies such as computed tomography (CT), magnetic resonance imaging (MRI), positron emission tomography (PET) and X-ray chest radiography [2] are available to assist radiologist. Although imaging tools such as CT and MRI are more precise and more sensitive, chest radiography remains the most common radiological procedure for the primary detection and diagnosis of lung nodules and makes up at least one-third of all radiological examinations [3]. Chest radiography is still the initial procedure, mainly because of its low cost, simplicity, and low radiation dose [2]. Detection and characterization of lesions at an early stage in chest radiographs is a complicated task for radiologists [4] due to the difficulties on the interpretation of images.

The development of computational systems to assist the radiologists in the interpretation of images, nodule detection and determination of their characteristics would ease these difficulties. Therefore, research on computer-aided diagnosis (CAD) of lung cancer in chest radiography became a popular area [5]. Typical computer-aided diagnosis system for lung cancer consists of several steps including pre-processing, nodule detection, nodule segmentation, feature extraction and classification.

The objective of this work is to develop a computer-aided diagnosis system to help the radiologists in the characterization of lung nodules. Our study involves comparing two different classification methods namely k-NN Classification and Fuzzy Rule Based Classification methods.

This introduction chapter aims to give information about the problem and solving approaches. In section 1.1 the statistical data on lung cancer in the world is given. The problems and usage of chest X-ray images is presented in section 1.2. Then, a

brief overview of computer aided diagnosis system in lung cancer studies are given in section 1.3. The earlier studies about CAD systems on lung cancer are explained in section 1.4. Finally, the overview of this thesis is in section 1.5.

1.1   Lung Cancer Statistics

Normally, cells have a controlled division and reproduction rate in order to provide a normal growth and repair the tissues. Cancer occurs when the cells start to multiply at an uncontrollable rate. Then the abnormal tissue masses develop which are called tumors. They can either be cancerous (malignant) or non-cancerous (benign) [6].

Lung cancer is one of the most common cancers in the world. In 2012, there were nearly 1.8 million new cases contributing 12.9% of the total. Among all types of cancer, lung cancer is the primary cause of death from cancer worldwide. There were approximately 1.59 million lung cancer-related deaths in the world in 2012, accounting for about 19.4% of the total [1].

Diagnosis of lung cancer at an early stage can improve the effectiveness of the treatment and it can increase the 5-yaer survival rate of the patients from an average of 16% up to 54% [7].Thus, improving the methods of diagnosing lung cancer in its early stages has a crucial importance.

1.2   Chest Radiography

A significant discovery which revolutionized the field of diagnostic medicine was the discovery of X-rays in 1895 by Wilhelm Conrad Röntgen [8]. X-rays are high energy radiation with waves shorter than those of visible light. Images obtained using low dose X-rays help diagnose disease. Film interpretations play an important

role on diagnostic evolutions. However, interpreting the chest radiographs for lung nodule detection is difficult even for experienced radiologists. Some of the factors that make the chest radiographs challenging to interpret are poor contrast, the wide scale of nodule sizes, the fluctuating intensities of nodules on radiographs (noise) and superimposed anatomical structures overlapping with regions of interest. According to studies, up to 30% of nodules in chest radiographs were missed by radiologists, even if the nodules were visible in retrospect. The reasons for that misdetection may be due to the differences in decision criteria, lack of clinical data limited time, lack of experience and anatomic noise on chest radiographs [9].

There is a normal PA (Posteroanterior) chest radiograph shown in Figure 1.1. The brightness at radiographs indicates absorbed radiation. Due to the fact that tissues absorb X-rays at different extents, the brightness on radiographs varies. A great amount of the lung area consists of air; therefore, they show up black in the image. Bony structures appear white and the other structures such as vessels, soft tissues and water appears at different levels of gray. As shown in Figure 1.1 several structures such as blood vessels, rib crossings or gases can seem similar to lung nodules because their representation is not unique. For instance, blood vessels appear as round objects on chest radiographs when they are at the same direction of the X-rays. Due to this, distinguishing the round objects from lung nodules becomes difficult. Moreover, another problem reducing the detection accuracy is that the chest radiographs may have poor contrast because of the noise in the image. The anatomic noise and quantum noise have a great influence on the image contrast. Anatomic noise occurs due to the projection of anatomic structures such as large blood vessels, ribs and lung tissue. The reason for the quantum noise, created by the imaging device, is the limited number of x-ray quanta [10]. There is another noise that arises from the imaging device called radiographic noise or image noise which takes place because of scattered radiation especially when a high kVp is used to get the image of a thick and large body part [11]. Moreover, because of the large area of the lungs, the contribution of scattered radiation to the images is increased.
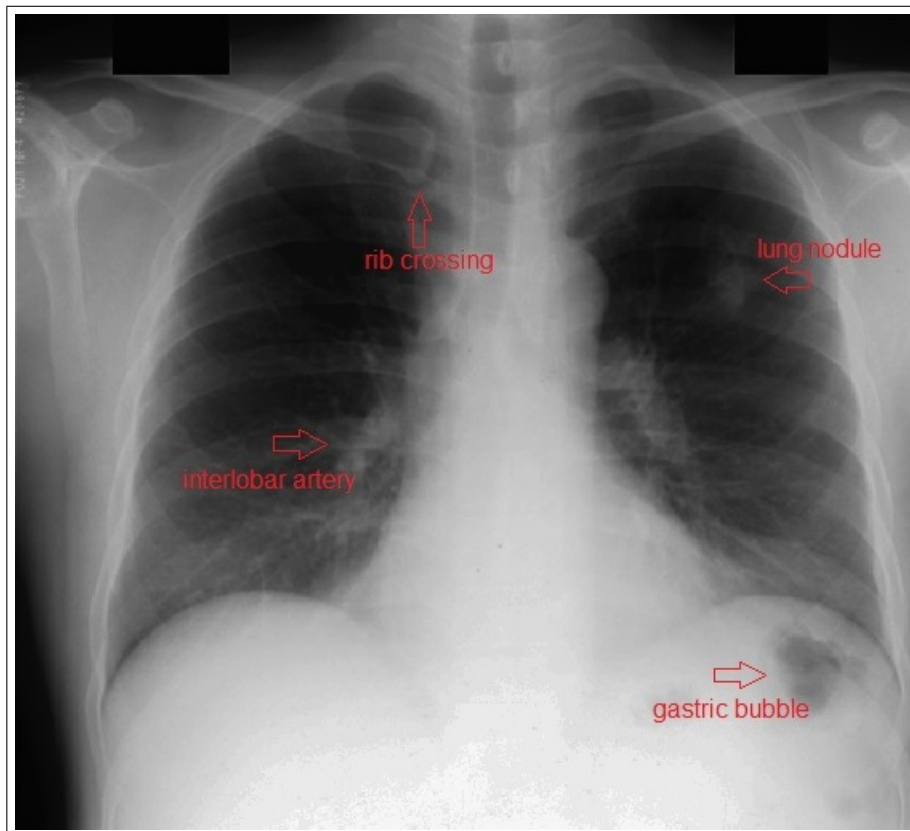
Figure 1.1 Example of a Posteroanterior chest radiograph

1.3 Computer Aided Diagnosis (CAD) Systems

After the invention of digital computer systems at the end of 1940s, research has been focused on the performance of computerized systems in tasks that had been performed by human previously. The advantages of these systems were the better effects in time, error rate and costs. In the case of lung nodule detection on chest radiographs early studies reported in the 1960s and 1970s, assumed that computers would replace radiologists in the diagnostic procedure [12]. However, the serious studies appear in the 1980s with the perspective of computer-aided diagnosis instead of automated computer diagnosis [12, 13]. These studies were not successful because access to digital images were hard, the advanced image-processing techniques were not existing and computers were not powerful enough [14]. In spite of the poor results, the first attempts had indicated that the computerized systems were aid the radiologists in terms of diagnosis accuracy [12, 15].

The main aspect of the computerized systems is to improve the performance of detection and diagnosis accuracy of cancer. The diagnostic type of CAD scheme is used for differential diagnosis of nodules based on classification between malignant and benign nodules. The most common studies have been done on the chest, breast and colon images [13]. The CAD systems that is developed to detect the breast cancer on mammograms is successfully used in clinical studies [14]. In terms of chest radiography the CAD systems have an important impact on the success of the image interpretation. Therefore, chest radiographs has become a popular area of research in medical imaging and diagnostic radiology.

There are five basic steps in the computer aided diagnosis schemes for diagnosis of lesions in chest radiographs. The flowchart for these systems is shown in Figure 1.2. The process starts with the detection of the lung nodules. The system contains the characterization of the detected nodules in terms of their malignancy. Firstly, the detected nodule areas are segmented and the features extracted from the segmented nodules. Then, according to the extracted features the nodules are classified as malignant or benign. Each of the steps explained in the further chapter in detail.

```
┌─────────────────────────────────────┐
│  ┌───────────────────────────────┐  │
│  │        Original Images        │  │
│  └───────────────────────────────┘  │
│                  ↓                   │
│  ┌───────────────────────────────┐  │
│  │       Detection of Lesions    │  │
│  └───────────────────────────────┘  │
│                  ↓                   │
│  ┌───────────────────────────────┐  │
│  │  Segmentation of Detected Lesions │
│  └───────────────────────────────┘  │
│                  ↓                   │
│  ┌───────────────────────────────┐  │
│  │        Feature Analysis       │  │
│  └───────────────────────────────┘  │
│                  ↓                   │
│  ┌───────────────────────────────┐  │
│  │ Diagnosis (Characterization) of Lesions │
│  └───────────────────────────────┘  │
└─────────────────────────────────────┘
```
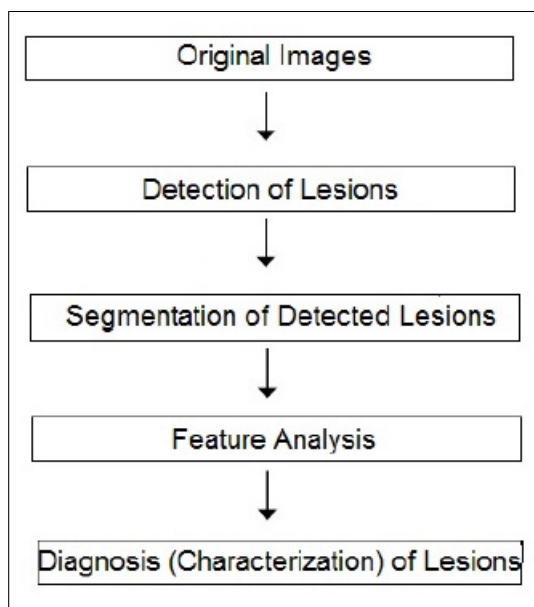
Figure 1.2 The flow chart of a typical CAD system

1.4 Literature Review

The task after segmenting a lung nodule on the chest radiographs is characterizing the lung nodules as malignant or benign. This process is challenging for radiologists. There are several studies on computerized systems which aim to provide a higher classification rate as a second decision. These methods are based on the analysis of features obtained from segmented nodule areas.

A group of researchers from The University of Chicago [16] presented a CAD scheme to compare the performance of radiologists and the developed system in determining the malignancy of nodules. The methods which are used to measure the malignancy are linear discriminant analysis (LDA) and artificial neural networks (ANN). The results of the study showed that the performance of the radiologists in the distinction between benign and malignant nodules was improved significantly by use of the computer output.

Patil et al. [17] proposed a study that aims to help the radiologists to identify the nodules in the early stage. In this method, texture feature estimation algorithms are applied to 147 chest x-ray images which consisted of small-cell (SC), non-small-cell (NSC) type and tuberculosis (TB) images. The features obtained from images by using image processing and analyzing methods were applied to an Artificial Neural Network (ANN) based classification system to classify the lung cancers into malignant and benign. As a result, the highest accuracy rate of the system is 83%.

Gindi et al. [18] reported a study where they have compared a Support Vector Machine (SVM)-based classifier with Euclidean distance classifier in case of curvelet texture extraction. The data set is contained 247 chest x-ray images from JSRT database. The result of this study demonstrates that the SVM approach yielded a better performance when compared to the Euclidean distance classifier. The correct classification rate for Euclidean distance classifier was 97% while the rate is 98.46% for SVM.

Suzuki et al. [19] presented a computer-aided diagnostic (CAD) scheme for distinction between benign and malignant nodules in low-dose helical computed tomography scans by use of a massive training artificial neural network (MTANN). The database contained 6 primary lung cancers in 73 patients and 413 benign nodules in 342 patients. The system correctly identifies 100% (76/76) of malignant nodules as malignant, while 48% (200/413) of benign nodules are identified correctly as benign.

Several studies have been conducted to compare the classification performance of the developed computerized schemes and radiologists. Some of the methods used for this purpose are multivariate logistic regression, Bayesian analysis and artificial neural networks [20].

Aoyama et al. [21] proposed a computerized method to assist radiologists for distinction between benign and malignant solitary pulmonary nodules on chest images. In the study, 55 chest radiographs are used. The location of a nodule is indicated first by a radiologist. The nodule is segmented automatically by contour lines of the gray-level distribution based on the polar-coordinate representation. Two clinical parameters, namely age and sex, and 75 image features are used to differentiate the benign and malignant nodule areas. The method used to assess the nodules on chest radiographs is artificial neural networks (ANNs). The performance of the proposed system and the manual system is compared in terms of the area under the ROC curves. According to the results, the performance of the proposed system is more efficient than the manual system.

The goal of the study presented by Shiraishi et al. [20] was to evaluate the performance of the radiologists in classifying lung nodules on chest radiographs with and without the use of CAD system. In addition to clinical features, computerized analysis of morphological features has been used for characterization. To determine the malignancy of the nodules linear discriminant analysis was applied. The results of the study indicated that the stand alone performance of the system was better than the performance of the radiologists. As a result, the study shows that the system has the potential to improve the classification accuracy of radiologists.

Recently, fuzzy logic based classification methods have been used for classification purpose.

Kaya et al. [22] developed a rule based fuzzy inference method to predict the malignancy of the lung nodules from computed tomography images. The dataset provided by Lung Image Database Consortium was used. The results are evaluated over classification accuracy performance and compared with single classifier methods. According to the results of the study, the classification accuracy of the fuzzy method reaches to 0.8328, while the accuracy of the k Nearest Neighbor method is 0.7959.

A computer aided diagnosis system has been reported by a research group from Kingston University and University of the Lausanne [23]. In this study, Fuzzy logic based classification have been used to classify the lung nodules. The aim of the study is to compare the performances of training algorithms. Mamdani Type and Sugeno Type fuzzy inference systems have been compared and evaluated in order to classify lung nodules. The results of the study show that the accuracy of the Mamandi type fuzzy inference system is 0.67212.

1.5   Organization of This Thesis

In this thesis, a semi-automatic computer aided diagnosis system has been developed in order to characterize the lung nodules which are obtained from the chest radiographs. The first chapter is the introduction. The second chapter is the materials & methods where the components of the developed system are explained in detail. In this part of the thesis the process starting with the pre-processing of the images is explained. At the end of the chapter the evaluation of the classification methods is given in terms of accuracy. The information about the database is also given in chapter 2. In the third chapter, the results of the classification process is given and discussed by comparing with the results of the other studies. The final chapter is the conclusion and future work. In this chapter, the study is summarized and the future work is presented.

2.   MATERIALS & METHODS

The overall scheme of our presented semi-automatic computer aided diagnosis system, shown in Figure 2.1, consists of five major steps: (1) Pre-processing of row chest radiographs, (2) Lung nodule detection based on template matching, (3) Lung nodule segmentation with the use of active contours, (4) Feature extraction from segmented nodule areas, (5) Classification of nodules based on extracted features by using Fuzzy rule based classifier and k nearest neighbor classifier. Each of the classification methods is evaluated in terms of their accuracy.

The nodule detection and nodule segmentation steps work semi-automatically. That means, if the automatic methods fail, the process is performed by the user, most probably by the radiologists.

This chapter provides a detailed description of the developed CAD system: the techniques and the results obtained from each stage. The chapter starts with the description of the database used in our system and then continues with the process of the CAD system respectively as given in Figure 2.1. Lastly, we discuss the classification methods.
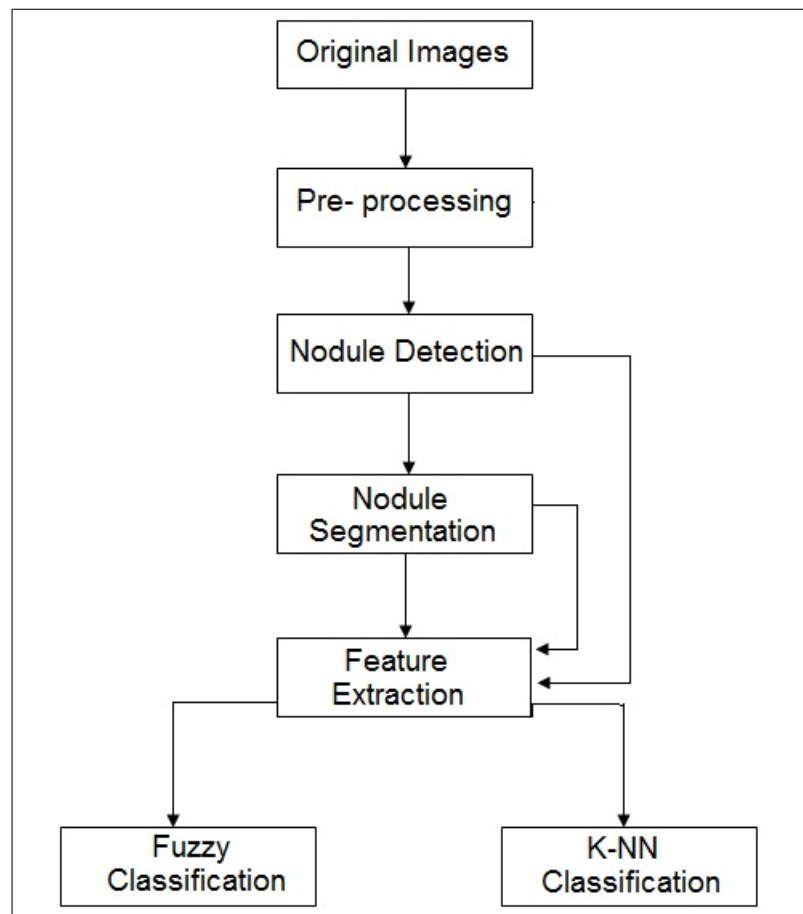
Figure 2.1 Processing flow of the developed CAD system

2.1 Database

The database which has been used in this study acquired by the Japanese Society of Radiological Technology (JSRT) and described in [24]. There is a text file given with the database which includes information about the nodules and patients such as nodule size (mm), age, sex, final diagnosis, degree of subtlety, anatomic location of the nodule, x and y coordinates of the center of the nodule in a digital image, and nodule classification as malignant or benign. The images were digitized with a 0.175 mm pixel size, a matrix size of 2048 by 2048, and 4096 gray levels corresponding to a 0.0-3.5 optical density range. There are 247 postero-anterior chest radiographs in the database, 154 with lung nodules (100 malignant and 54 benign) and 93 without a nodule. Out of 154 lung nodules, 31 nodules size between 0-10mm, 52 nodules size

between 11-15mm, 36 nodules are between 16-20mm, 14 nodules size between 21-25 mm, 17 nodules size between 26-30mm and, finally, 4 nodules size between 31-60 mm. The average size of the nodules is 17.3 mm. The images with nodules were classified by three chest radiologists according to the degree of subtlety of the lung nodules. The groups are as the following: level 1, extremely subtle; level 2, very subtle; level 3, subtle; level 4, relatively obvious; and level 5, obvious. At level 1, detecting the nodules is extremely difficult due to low contrast, small size or the nodule overlapped with a normal structure. When it comes to level 5, the detection is relatively easy. 25 images with nodules were categorized as level 1, 29 images as level 2, 50 images as level 3, 38 images as level 4, and 12 images as level 5.

2.2   Pre-Processing

The aim of the pre-processing step in the system is to improve the quality of the images in order to increase the success of the other process. The pre-processing techniques deal with enhancing contrast, removing noise and correct the effects of patient motion on images. This step is very crucial because the images contain a lot of irrelevant information.

Contrast enhancement is an important aspect for image visuality. Contrast is determined by the difference in the brightness of a region with the background brightness. Human visual system is sensitive to contrast [25]. Therefore, improving the contrast of the images has a crucial importance especially in medical imaging. The reasons for low contrast in x-ray images are poor illumination, lack of dynamic range in the imaging sensor and wrong settings of a lens aperture during image acquisition [26]. Some of the commonly used methods for contrast enhancement are histogram equalization and contrast stretching. The goal of the contrast stretching technique is to increase the dynamic range of the gray levels. In our study, we have used histogram equalization in order to improve the contrast of the images.

X-ray images commonly include Gaussian noise and salt and pepper noise. This

type of noise, which arises due to the decoding errors in picture transmission systems, can appear as white and black points on the image [25]. In order to remove this noise low pass filtering is used [27]. We have used median filter to remove the irrelevant noise on the chest radiographs.

The raw chest radiographs in the database have resolutions of 2048x2048 pixels with a grayscale of 12 bits. In this study, the matrix size was reduced to 512x512 by sub-sampling of the original image data by a factor of 4 for a faster computational process. However, the grayscale remains as the same because the resolution is a crucial property for image processing. The higher resolution provides the more detailed images.

2.2.1 Contrast Enhancement by Histogram Equalization

The histogram of an image determines the frequency distribution of image gray levels. For 12 bit pixels, the brightness range changes from zero (white) to 4095 (black). The intensity levels in between them are the gray shades for an image. To have equal number of pixels in all the gray levels is an indication of a visually perfect image. The histogram equalization method provides to improve the image quality by equally distributing pixel intensity throughout the available gray scale [28]. The equation for histogram equalization is given below.

$$k = \sum_{i=0}^{j} \frac{N_i}{T} * I_{max} \qquad (2.1)$$

where k is the new intensity value of the corresponding brightness level j in the original image, N_i is the number of pixels with brightness values i, I_{max} is the maximum pixel intensity value, and T is the total number of pixels in the image.

The original chest image and its histogram is shown in Figure 2.2 and Figure 2.3 respectively. Figure 2.4 and Figure 2.5 show the image after equalizing the histogram and its histogram. Histogram equalization improves the relative contrast of the image.
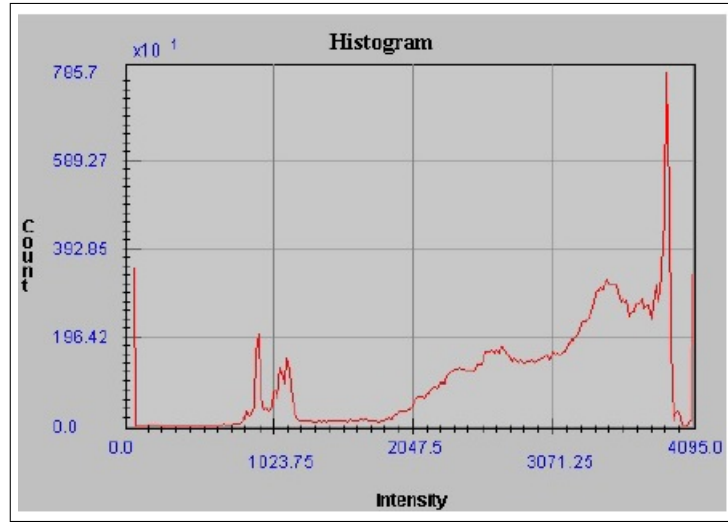
Figure 2.2 The original image

Figure 2.3 Histogram of the original image

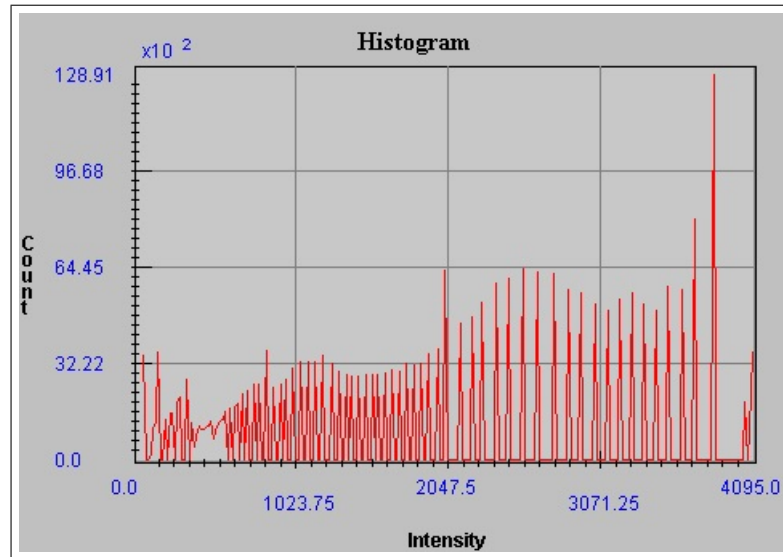**Figure 2.4** Histogram equalized image

Figure 2.5 Histogram of the image after histogram equalization

2.2.2   Noise Reduction by Median Filter

After improving the contrast of the original chest radiograph, we have applied median filter in order to remove the salt and pepper noise on the images. The principle of the median filtering is to remove the pixel value (gray level value) of a target pixel with the median value of its neighborhood as shown in Figure 2.6. The original value of the pixel is also included while finding the median value. Median is the middle value of a rank ordered set. An example in order to find the median value of a 3x3 matrix is given in Figure 2.6. In this study, we have used a filter in 5x5 neighborhood. In this case, the median value is the 13th largest value.
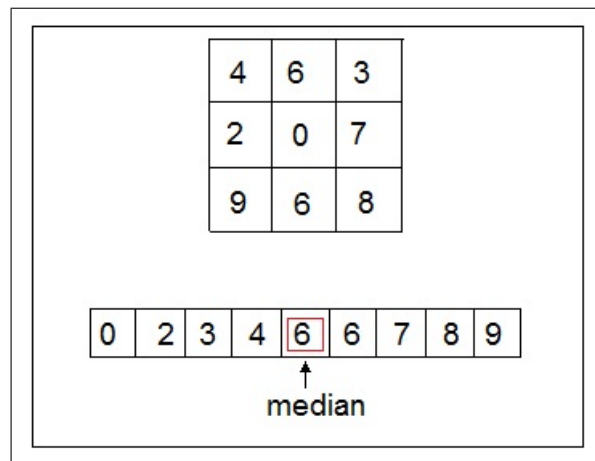
Figure 2.6 The principle of median filter

There are several advantages of median filters over the linear smoothing filters. For instance, they provide less blurring while removing the noise significantly. Moreover, the edges and large changes in image intensity are not affected in terms of gray level intensity which has a crucial importance during the segmentation process on chest radiographs [29].

The image after applying 5x5 median filter is shown in Figure 2.7.

Figure 2.7 The filtered image

2.3 Lung Nodule Detection

The detection of lung nodules on chest radiographs is the most studied problem in computer analysis, for the early detection has a crucial importance in increasing the patient's chance of survival. However, it is difficult to distinguish nodules from overlapping structures on the lung area such as vessels, ribs and heart. Therefore, detection methods for lung nodules are usually applied after preprocessing.

The techniques which have been reported for nodule detection are: multiple gray-level thresholding, mathematical morphology, genetic algorithm template matching of Gaussian spheres, clustering, connected component analysis, thresholding, detection of circles, gray-level distance transform and filters enhancing structures [30].

In this study, we have developed a scheme based on template matching techniques in order to detect the pulmonary nodules automatically in chest radiographs. In addition to the automatic detection process, a manual detection option has been added to the system in order to determine the lesions when the automatic system has failed.

In this section, the detection methods which we have used were explained in detail.

2.3.1   Template Matching for Lung Nodule Detection

Template matching is a process that is used to find a specific object from the image by matching a model image. This model image is a sub-image which contains the shape of the target object. Similar template matching techniques for nodule detection have been used previously by Lee et al. in [31] and by Li. Et al. in [32].

The nodules in the chest x-ray images used in this study are all less than 30 mm, with the exception of four nodules that were between 31mm and 60mm. In general, nodules in the lung area tend to have circular shapes [31]. Therefore, to recognize these nodules, we used four circular templates with Gaussian distribution, shown in Figure 2.8. The diameters of the models are 10, 20, 30 and 40 pixels (one pixel 0.7 mm), respectively. Using these four models, we expect to detect nodules having diameters of approximately 5-30 mm.
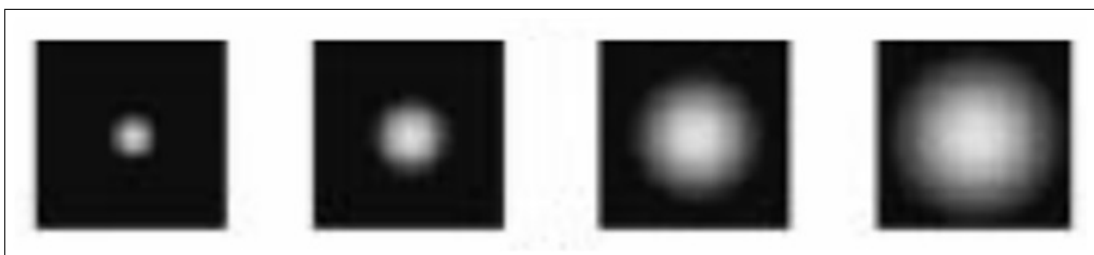

Figure 2.8 Template for lung nodules

The nodular models were determined by the following equation [31]:

$$P_{xy} = me^{-(x^2+y^2)/n} \tag{2.2}$$

where P_{xy} is the pixel intensity of the x, y coordinate, m is the maximum value of the distribution and n is the variance of the distribution. These values were determined experimentally in order to maximize the detection rate.

A conventional template matching was applied to detect the nodules on the chest X-ray images. The degree of matching between the image and the template is described by normalized cross-correlation coefficient as given in Eq.2.3 [25].

$$\max e = \frac{\sum(I_{x+i,y+j} - \bar{I}_{i,j})(T_{x,y} - \bar{T})}{\sqrt{\sum(I_{x+i,y+j} - \bar{I}_{i,j})^2(T_{x,y} - \bar{T})^2}} \tag{2.3}$$

where $\bar{I}$ is the mean of the pixels $I_{x+i,y+j}$ for points within the image (i.e. $x, y \in W$) and $\bar{T}$ is the mean of the pixels of the template.

The result of the equation varies from 0 to 1 which gives the matching degree. The cross-correlation coefficient value gets close to 1 where the template best matches with the object on the chest radiograph. The result depends on the shape of the intensity value distribution in both the original image and the template image.

As a result, the maximum correlation values between the nodular models and the chest images were selected from the given formula. According to these values a detection threshold was determined. If the correlation value exceeds the given threshold then the matched area is taken as a suspected nodule area. The x, y coordinates of the center of the matched area was obtained and labeled as shown in Figure 2.9. Since the nodule areas do not have a perfectly circular shape, a nodule segmentation process was applied to specify the borders of the nodules after detection process. Therefore, the suspected nodule areas were enclosed by a circle where the radius of the circle was determined according to the size of the template image in order to cover the whole
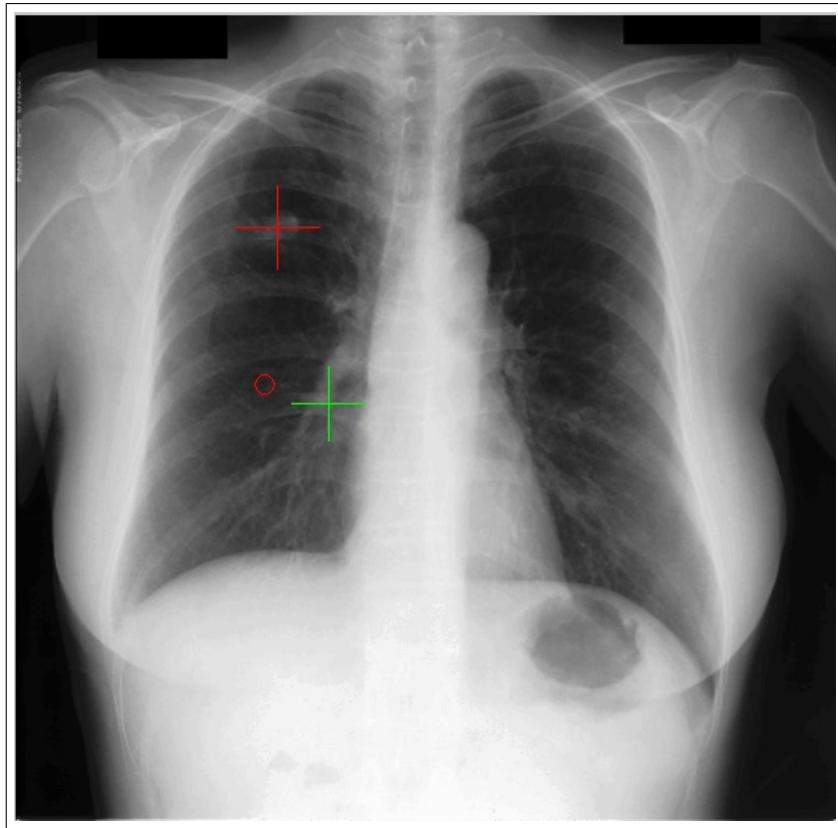
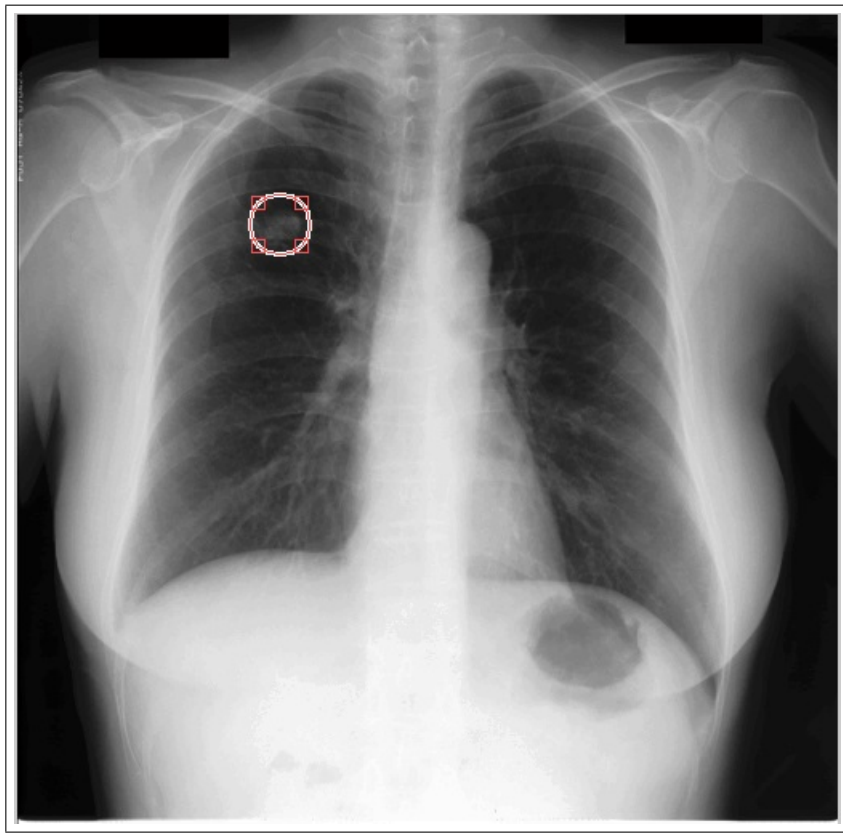nodule area as shown in Figure 2.10.

Figure 2.9 Suspected nodule areas

Figure 2.10 Labeled nodule area

2.4   Lung Nodule Segmentation

Segmentation is a process used in order to divide the images into multiple mean-ingful parts which are more specific and easier to analyze. The nodule segmentation part has a crucial importance on computational applications. During this procedure the boundaries of the lung nodules are improved, because the features can be extracted for further stages from the delineated nodule area such as malignancy classification. The accurate segmentation of the nodule areas improves the quality of the extracted features and, as a consequence, the success of the classification task.

According to the review study which has been done by El-Baz et al. [33] the reported lung nodule segmentation methods are (1) thresholding, (2) mathematical morphology, (3) region growing, (4) deformable model, (5) dynamic programming, (6) spherical/ellipsoidal model fitting, (7) probabilistic classification, (8) discriminative classification, (9) mean shift, (10) graph-cuts, and (11) watersheds.

We have built a semi-automatic method for lung nodule segmentation. The initial attempt is to determine the nodule border automatically. Then, if the automatic system do not work properly, the radiologists segment the nodules manually from a screen that contains four version of the same chest x-ray image which are: the original image, the image after pre-processing, a pseudo-colored image and the image after applying fuzzy minimization.

We have developed a two-stage method to segment the nodule automatically. The first stage of the process contains procedures in order to improve the nodule border to ease the segmentation. The second stage is to delineate the nodule areas by using active contours which is a part of dynamic programming method according to the mentioned review study.

In this section, the automatic and manual segmentation processes are explained in detail.

2.4.1   Automatic Nodule Segmentation Process

In this study, the automatic nodule segmentation process consists of two main steps. The aim of the first step is to improve the borders of the nodules in order to increase the correctly segmented nodule rate. The second part is to delineate the area with active contours.

We have used an image from the database as a reference image in order to determine the characteristics of the process. Firstly, we have applied the histogram normalization according to the minimum and maximum gray level values of the reference image in order to obtain the same interval for all of the images. Secondly, we have set the window/level of the reference image to optimize the best value where the lesion distinguished from the background as clear as possible. Then, we have applied the fuzzy minimization algorithm which eliminates the irrelevant background. After fuzzy minimization, the active contour has been used. Finally, the intensity of the area out off the segmented nodule area set to zero. The final segmented nodule area has been used for feature extraction process.

Histogram normalization is a technique where the intensity interval of the images is changed to stretch the gray level. The minimum intensity value of our reference image is 191 while the maximum value is 3167. We have set the intensity range to 191-3167 for all of the chest radiographs in the database due to get normalized images. The equation for histogram normalization is given below.

$$N_{x,y} = \frac{N_{max} - N_{min}}{O_{max} - O_{min}}(O_{x,y} - O_{min}) + N_{min} \tag{2.4}$$

where, O_{min} and O_{max} are the minimum and maximum gray level values of the original image and N_{min} and N_{max} are the values of the reference image.

After histogram normalization, we have changed the window/level of the reference image. Here, the goal is to obtain the maximum detectability of the nodule

area by eliminating the background structures which is, in our case, the irrelevant lung areas such as ribs.

The windowing makes it possible to enhance the contrast of the image in a specific area of the intensity range. For instance, a higher contrast can be achieved in the darker areas or in the brighter areas of the chest images. The window and level of the reference image are 2046 and 4094 respectively as shown in Figure 2.13. We have changed the values to 1024 and 3011 in order to increase the visibility of the lesion as shown in Figure 2.13.
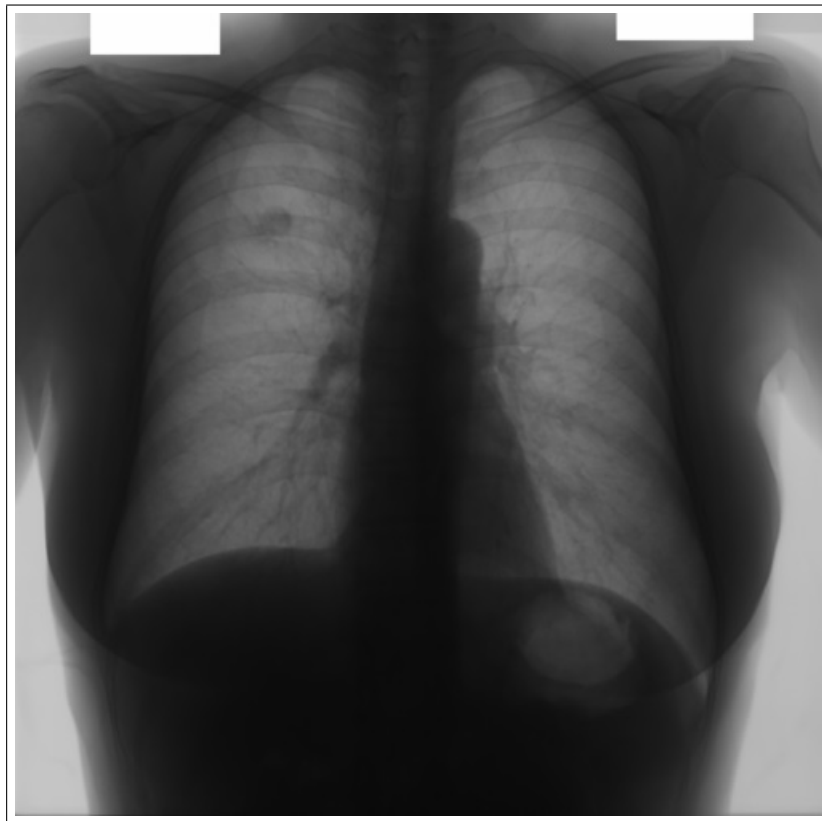
Figure 2.11 The original image
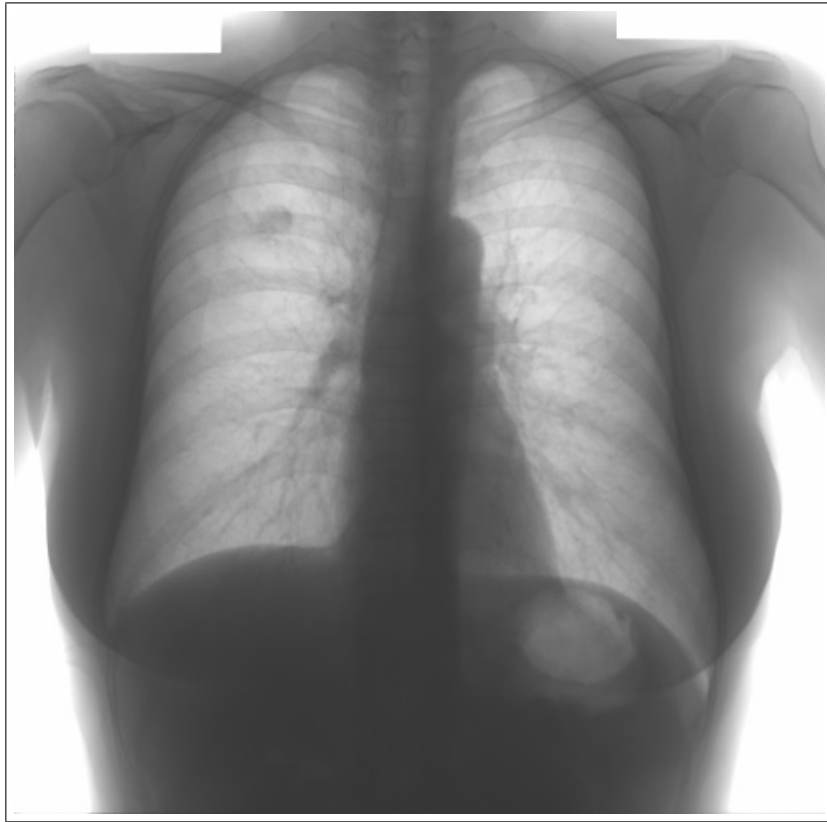
Figure 2.12 Image after setting window/level
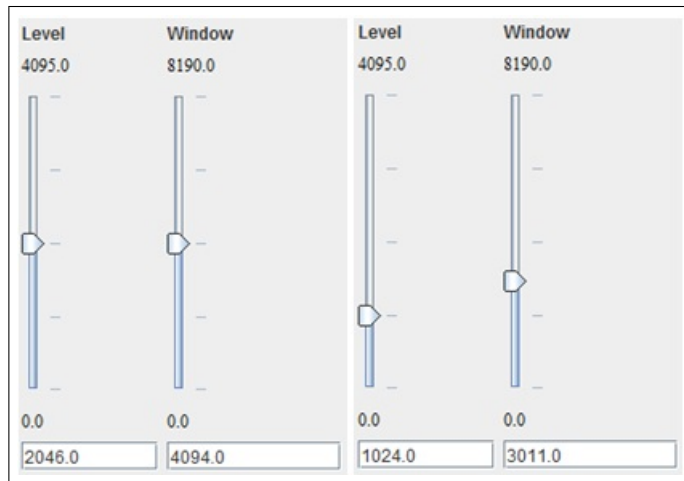
Figure 2.13 Window/level values of the original image and the image after process

The main purpose of the fuzzy minimization process is the image enhancement by reducing the amount of the fuzziness of the image. The algorithm follows mainly three steps which are (1) Gray-level fuzzification, (2) Membership modification and (3) To determine the new gray-levels by defuzzification [34, 35].

The image after fuzzy minimization is shown in Figure 2.14 and the inversion applied image is shown in Figure 2.15. The difference between the two images is only the opposite gray level which means that the pixel values of the black and white regions are replaced. They do not have a difference in terms of the contrast or other properties.

Figure 2.14 Image after fuzzy minimization

Figure 2.15 Inverted image

To delineate the lung nodule boundary active contours, also called as snakes, have been used. It is one of the most common techniques used for automatic segmentation purposes. The aim of this method is to describe a target area by enclosing it, which is the perimeter of the nodule in our study. To start the process an initial contour is positioned outside of the nodule. Then, the contour is minimized until it matches the target perimeter.
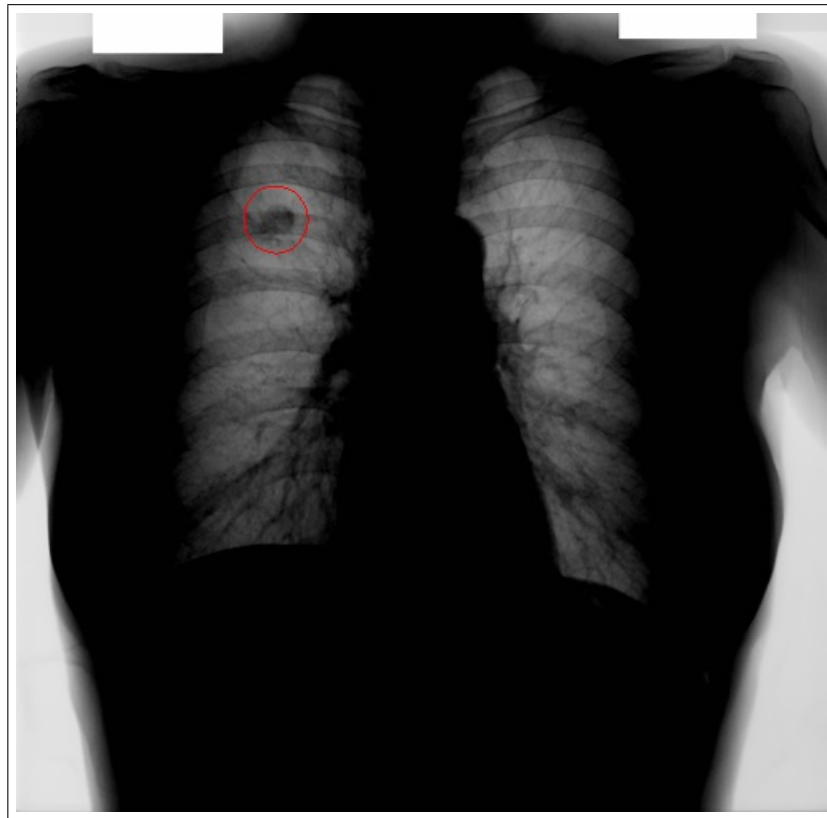
The method is proceeded as an energy minimization based on the Eq.2.5 where E_{int} is the internal energy of the contour, E_{image} is the energy of the image , E_{con} constrained energy of the image which are functions of the points that creates a snake v(s) (x and y coordinates of the snake).

$$E_{snake} = \int_{s=0}^{1} E_{int}(v(s)) + E_{image}(v(s)) + E_{con}(v(s))ds \qquad (2.5)$$

where E_{int} conducts the order of the snake points, E_{image} and E_{con} provide low-level and detailed information respectively to control the approach of the snake to the target contour. The acquired snake contour has a lower energy and higher match with the nodule boundary [25].

The initial contour has been determined according to the template area after template matching process. It can be stated manually by the user. The initial boundary and the minimized boundary which enclose the nodule area on the image after applying fuzzy minimization algorithm is shown in Figure 2.16.

After determining the nodule boundary, the nodule area have been extracted by setting the outer area to zero which is equal to a black background. Then, this segmented nodule area have been used to extract features to use in characterization of the lung nodules. The segmented nodule area is shown in Figure 2.17.
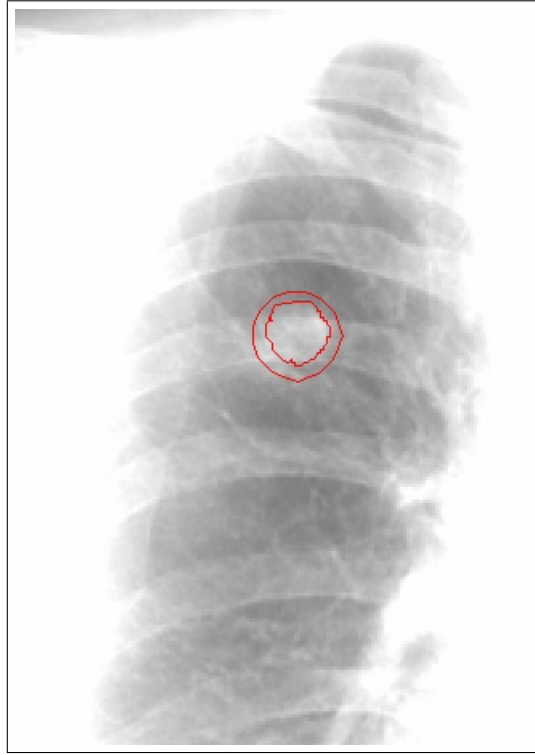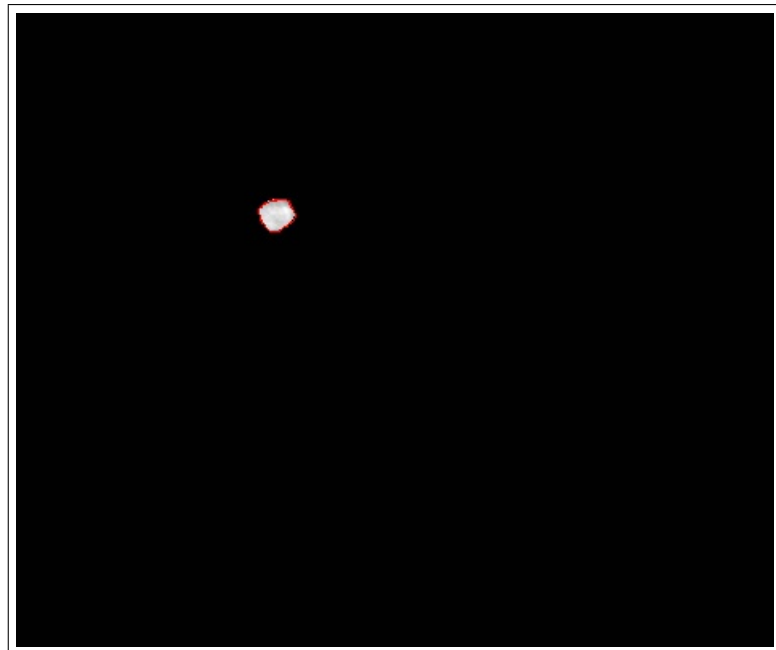
Figure 2.16 Active contour

Figure 2.17 Segmented nodule area

2.4.2 Manual Nodule Segmentation Process

The manual lung nodule segmentation procedure is used to delineate the lung borders by the user when the automatic process failed. We have developed an interface in order to increase the success of the segmentation. The system involves four different versions of the chest radiographs, which are the original image, the pre-processed image, the image after fuzzy minimization process and the colored image. The novelty of this divided screen is to give the opportunity to compare the nodule borders from a different view.

The raw chest x-ray images can contain noise and low contrast particularly when there are overlapped structures. Therefore, we have added three different processed images of the original image. As mentioned before in pre-processing part, the pre-processed image was obtained from the raw image after contrast enhancement and noise reduction. Thus, the nodule area is expected to be more detectible after this process. The fuzzy minimization provides a simpler image than the original one by removing the fuzziness of the image. Thus, the border of the nodules can be seen more clearly. However, some nodules such as the nodules close to the lung borders can become invisible after fuzzy minimization. Lastly, we have added pseudo color to the chest images in order to offer a visibly different image to the human vision. We have used MATLAB to colorize the grayscale image. The principle of this algorithm is to add color according to gray level of the pixel.

The images used for the manual segmentation process is shown in Figure 2.18 where the nodule area is labeled.

Some parts of the lung nodule boundary can be more visible at different images. Thus, we have added simultaneous zoom and bordering properties to the system due to allow the users to compare the four images at the same time. Our aim is to make the segmentation process easier and more effective for users. This interface is shown in Figure 2.19.
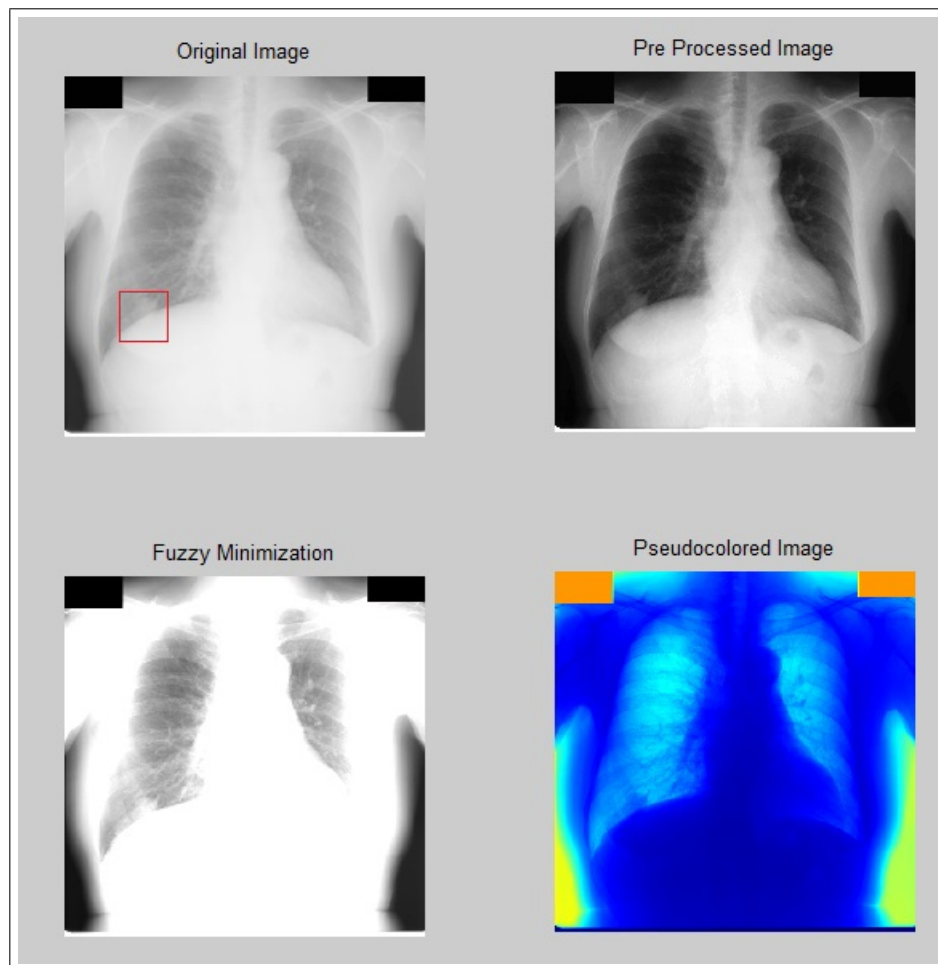
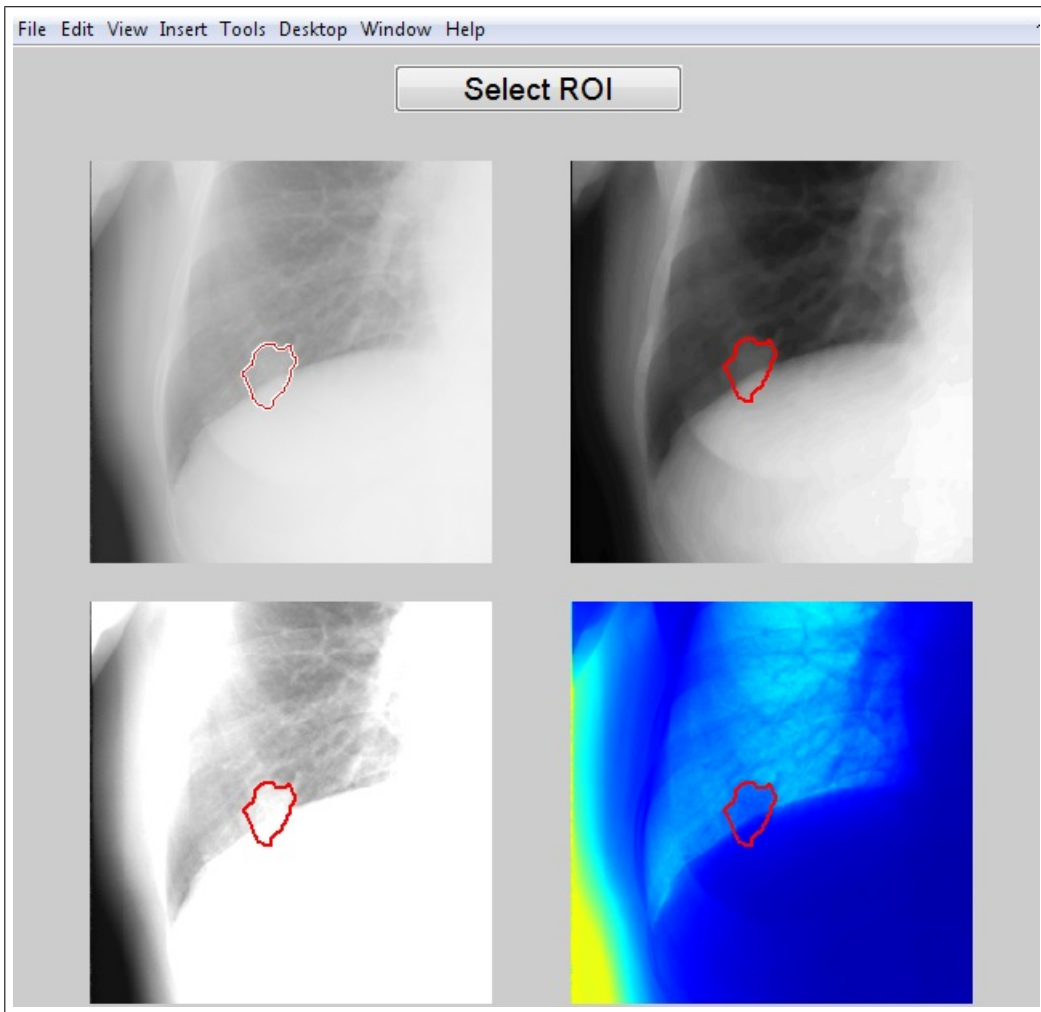**Figure 2.18** The images used for manual segmentation

Figure 2.19 Manual segmentation interface

The multiple image delineation process for manual nodule segmentation has been discussed with Dr. Hıdır Kaygusuz from Dr. Abdurrahman Yurtaslan Ankara Oncology Training and Research Hospital. Randomly chosen 30 images have been evaluated. Firstly, the nodule areas were segmented from the raw chest radiographs by the radiologist. As a result, 19 nodules were delineated properly; the segmentation rate was 63.3%±17.2. Secondly, the segmentation for the same 30 images has been performed by using the multiple screen. In this situation, the number of correctly segmented nodules increased to 24 which is 80%±14.3 of all. As a result, the segmentation rate has been increased at a rate of 16.7% with the help of the multiple delineation option.

2.4.3   Results of Nodule Segmentation

The automatic segmentation process failed in some images. The main reasons for this failure are the low visibility of some images, the nodules which lay under the other structures of the chest such as the heart. Moreover, some nodules become invisible after applying fuzzy minimization due to their positions near to the lung borders. These nodule areas have been extracted semi-automatically or manually by the users. The manually segmented nodules are mostly included in the level 1 according to their degree of subtlety.

We have used 154 chest x-ray images which have 154 nodule areas in total. The numbers of the nodules according to their segmentation process is shown in Table 2.1.

2.5   Feature Extraction

The features give information about the characteristics of the object which can be defined as the measurable properties of an image. Therefore, feature extraction is one of the most important parts of the CAD system which helps the system in

Table 2.1
The number of segmented nodules according to the method.

	Segmentation Process		
	Automatic	Semi-automatic	Manual
# segmented nodules	78	26	46

characterizing the nodules. The features obtained from the segmented nodule area indicate information related to the lung nodule which enables the system to classify the nodules as malignant or benign [36]. In this work, several features are calculated from the segmented nodule areas by using MATLAB. They are mainly three features: geometrical, statistical and textural. The features have been selected according to the previous studies which have been done by Lingayat et al. in [37] and by Patil et al. in [36].

2.5.1 Geometrical Features

Geometrical features are shape-based characteristics of the objects. The variation between the segmented nodule areas provides an effective classification. The geometrical features used in this study are area, perimeter, circularity (irregularity index), equivalent diameter, convex area and solidity are obtained from the binary image which consists of ones and zeros as shown in Figure 2.20 and Figure 2.21.

Area

Area is the number of pixels in the image array. In the binary images, the number of ones is counted to find the area of the nodules because in the binary image the nodule area consists of ones and the outer area consists of zeros.

$$A = n[1] \tag{2.6}$$
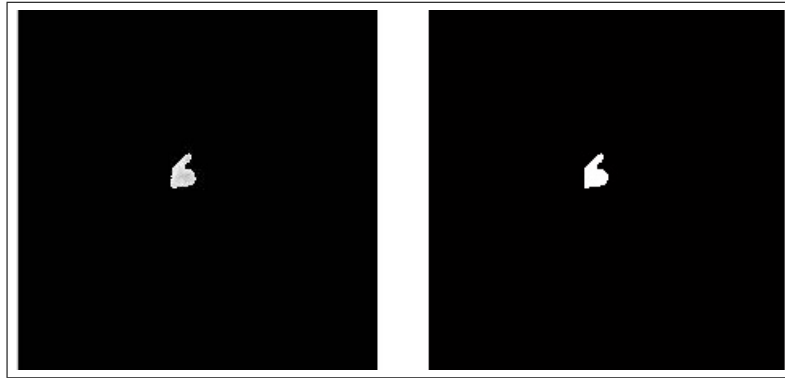
Figure 2.20 Segmented area of a malignant nodule

Figure 2.21 Segmented area of a benign nodule

Perimeter

Perimeter is the distance around the object. In MATLAB, this property of the nodule area is calculated by counting the pixels around the boundary of the nodule.

Circularity

The circularity of the nodule indicates the growth of the nodule which is a crucial parameter in specifying the malignant nodules [38]. The degree of irregularity around the boundary of the nodule is defined by an index that is calculated as the following:

$$I = \frac{4\pi Area}{perimeter^2} \tag{2.7}$$

The value of the index is equal to 1 if the object is circular. Otherwise, the value is less than 1 [39]. It is assumed that the probability of the existence of a nodule increases in direct proportion with the circularity [36].

Equivalent Diameter

Equivalent diameter is the value of the diameter of a circle which has the same area as the object. The formula given for calculating equivalent diameter is:

$$E_{diameter} = \sqrt{\frac{4Area}{\pi}}$$

(2.8)

Convex Area

The value of the convex area is calculated by counting the pixels of convex image which is the smallest polygon that contains the nodule region.

Solidity

The solidity is explained as the correlation between the convex area and the area of an object. For very irregular surface, solidity comes near to 0 values. The formula of solidity is given as the following:

$$Solidity = \frac{Area}{Convexarea}$$

(2.9)

2.5.2 Textural Features

Texture is an important property of images which is capable of differentiating textural images from non-textural images. Moreover, textural properties are more effective in classification when they are used with other attributes.

One of the methods to extract the textural features is to obtain the features

from gray-level co-occurrence matrix statistically. GLCM counts the co-occurrence of pixels with gray values at a given distance and direction [40]. To determine the texture of an image with a single offset is difficult. Thus, we specified offset values at 0° [0 1], 45° [-1 1], 90° [-1 0] and 135° [-1 -1] as shown in Figure 2.22.
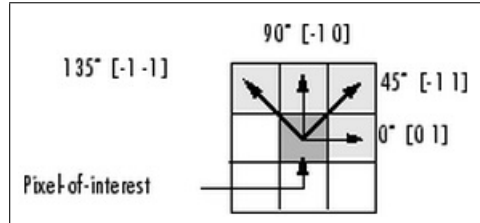
Figure 2.22 GLCM with different offsets

The textural features calculated in this study are: contrast, correlation, energy and homogeneity. The formulas related to these properties are given below. i and j values in the equations stand for the coordinates of the pixel in the image.

Contrast

$$contrast = \sum\nolimits_{i,j} |i - j|^2 p(i,j) \tag{2.10}$$

Correlation

$$correlation = \sum\nolimits_{i,j} \frac{(i - \mu i)(j - \mu j)p(i,j)}{\sigma_i \sigma_j} \tag{2.11}$$

Energy

$$energy = \sum\nolimits_{i,j} p(i,j)^2 \tag{2.12}$$

Homogeneity

$$homogeneity = \sum\nolimits_{i,j} \frac{p(i,j)}{1 + |i - j|} \tag{2.13}$$

2.5.3   Statistical Features

A frequently used approach for describing a region is to quantify the statistical properties. These properties are calculated as an indicator of the gray level of the images.

The statistical features calculated in this study are: entropy, mean, variance and standard deviation. The formulas related to these properties are given below. Where i and j are the coordinates of the pixel in the image, M and N are the total number of pixel in the row and column.

Entropy

Entropy measures the randomness of a gray-level distribution.

$$E = -\sum_{i}^{m} \sum_{j}^{n} P[i,j] \log P[i,j] \tag{2.14}$$

Mean

$$\mu = \frac{1}{N \times M} \sum_{i=0}^{M} \sum_{j=0}^{N} P(i,j) \tag{2.15}$$

The mean value of the gray levels in the image is calculated by the formula given below.

Variance

$$\sigma^2 = \frac{1}{N \times M} \sum_{i=0}^{M-1} \sum_{j=0}^{N-1} (P(i,j) - \mu)^2 \tag{2.16}$$

It is a statistical measure of spread or variability. The variance is large when the gray levels of the image are spread out greatly.

Standard Deviation

$$std = \sqrt{\sigma^2} \qquad\qquad (2.17)$$

We calculated 14 features from each of the segmented nodule areas. The values of extracted features from the nodule areas are given in Table 2.2 for a benign and a malignant nodule.

Table 2.2
Feature values for benign and malignant nodules.

Feature	Benign	Malignant
Area	92	65
Perimeter	38,38478	77,59798
Convex Area	99	321
Solidity	0,929293	0,825545
Equivalent Diameter	10,82303	18,36868
Circularity	0,784657	0,553038
Entropy	0,004534	0,011516
Mean	0,000351	0,001011
Standard Deviation	0,01873	0,031779
Variance	0,000351	0,00101
Contrast	0,005309	0,010393
Correlation	0,826197	0,868111
Energy	0,999109	0,997656
Homogeneity	0,999809	0,999617

2.6   Classification

The purpose of CAD for classification and radiologic evaluation of nodules on chest radiographs is to noninvasively differentiate benign from malignant lesions as accurately as possible. Several studies have been reported related to lung nodule characterization. Some of the methods used for this purpose are multivariate logistic regression, Bayesian analysis, artificial neural networks [20], support vector machines and fuzzy inference systems.

In this study, we have used two classification methods separately which are k Nearest Neighbor Classification and Fuzzy Rule Based Classification to compare their performance. In this section, these methods are explained in detail.

2.6.1   K-Nearest Neighbor Classification

The k nearest neighbor (k-NN) is one of the most commonly used classification methods because of its simplicity. The basic concept of the model is to predict the class of the object on the classes of its k nearest neighbors. According to the majority of these neighbors the class of the object is specified [41]. To make a classification, the optimal number of the nearest samples (k value) is determined experimentally for un-supervised learning. Moreover, for supervised learning it is learned during cross-validation [42]. The nearness indicates a distance metric which by default is the Euclidean distance. Euclidian Distance (d) is defined as given below where s and k are any two images and M is the number of features [25].

$$d = \sqrt{\sum_{i=1}^{M}(s_i - k_i)^2} \tag{2.18}$$

There is a simple instance shown in Figure 2.23. There are samples of two classes namely, class A and class B, and an unknown sample which is wanted to be classified. The members of class A and class B represented by X and O, respectively.

According to this example, x1 and x2 are the features of samples. In this situation, if the k value is 3, the nearest three neighbors are selected (those three with the least distance) and as a result the sample belongs to class B. In contrast, when the k value is 5, the sample belongs to class A.
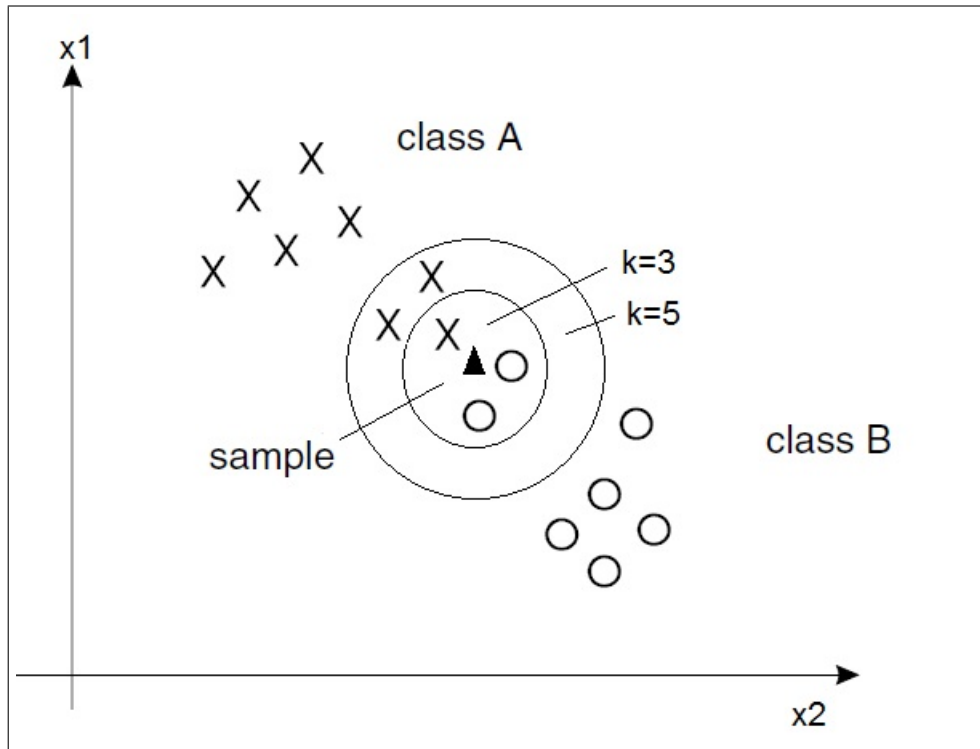
Figure 2.23 Example of k-NN classification

In the present study, the k-NN classifier was trained and tested with a leave-one out cross-validation test. LOOCV method consists of training a classifier using all samples except for one. Then, this left-out sample is used to test the system. This process continues until all of the samples have been classified. The percentage of correctly classified samples gives the LOOCV accuracy. LOOCV is commonly used when the number of samples is limited [42].

Our data set consists of 154 images, 100 of them contain malignant and 54 of them contain benign nodule areas. As explained in Feature Extraction section, we measure 14 features from all of the nodule areas. We apply k-NN classification method to classify these 154 images as benign or malignant by using the measured features.

In this study, we have used MATLAB to implement the k-NN classification method. To apply this method we have determined a training set, the group of the each data in the training set, a sample data and the k value. Firstly, we have divided the images in the data set into two classes namely class 1 and class 2 which depicted malignant and benign nodules respectively. These labels constitute to the group variable.

Moreover, we have developed an algorithm to apply leave-one-out cross validation method to determine the training data set and test data for classification. The aim of using this method is to use all of the samples as training data. According to this algorithm each of the samples have been used as test data one by one and classified as malignant and benign. Lastly, we have specified the characteristic of the classification method by setting an initial k value and determining the distance metric as Euclidian distance.

To optimize the method we have tested the system with several k values. The evaluation metric used in this study is classification accuracy. Thus, we set several k values to get the higher accuracy. The k values which are used to optimize the procedure are 5, 15, 25, 30, 35, 40 and 60. The higher classification accuracy (68.8%) have been obtained when the k value have set to 30.

When we eliminate, the textural features (contrast, correlation, energy and homogeneity), the accuracy rate at every k value have remained as the same. Thus, we have not used these features at classification procedure to reduce the complexity of the algorithm and the computational load which provides a faster classification.

2.6.2 Fuzzy Rule Based Classification

The computers work with strings 0 and 1 while the human knowledge is not as precise as computer systems. The judgments of natural language are partially true or false because of the lack of information and limitation in defining knowledge. To

deal with this uncertainty, the fuzzy logic structures are developed which are closer to human reasoning than the present day computers. One of the most common application areas of fuzzy logic is data classification. In this study, we have used the fuzzy logic based classification system to classify the lung nodules as malignant or benign.

In contrast to classical theory, in fuzzy logic based classification the object can be partially in a class. The classical systems have only two membership degrees either 1 or 0 which means that the object is entirely a member of the class or not. On the other hand, in fuzzy classification, the membership values vary between 0 and 1, one constitutes to the object that belongs to the class, while zero is the opposite and other values between them gives the membership degree of being in the class. Fuzzy set theory represents the linguistic perspective and rules which provides a model to human knowledge.

The fuzzy inference systems are rule-based systems that make the decisions dependent on the rules. The basic form of the rules is "IF X is A THEN Y is B" where X and Y are fuzzy sets. The if-part of the rule "x is A" is called the antecedent while the then-part of the rule "y is B" is called the consequent. The fuzzy rules are more understandable and easier to change than the classical rules [43].

There are two important types of fuzzy inference methods: Mamdani's fuzzy inference method and Sugeno method. We have used the Mamdani's method for this study. Mamdani's method is the most commonly used method and it has widespread acceptance. Moreover, other advantages of this method are: being intuitive and suitable to human decisions [49]. A Mamdani type fuzzy inference system mainly consists of four parts: fuzzifier, knowledge base, decision making unit and defuzzifier [44]. A standard model for this type of fuzzy system is shown in Figure 2.24.
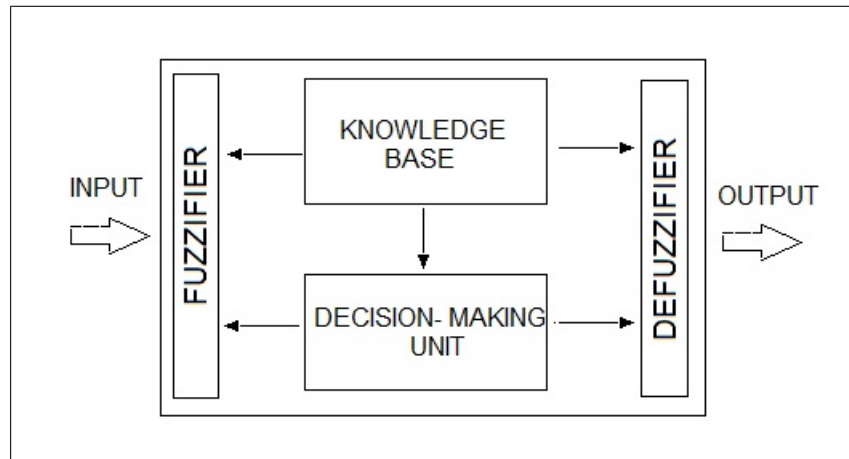
Figure 2.24 Block diagram of the Fuzzy inference System

The system contains both the antecedent and consequent parts of the rules. Therefore the form of the IF-THEN rules is as follows:

IF A1 is X1 and/ or ...and/ or An is Xn THEN B is Y [43].

where Ai and B are input and output variables and Xi and Y are the linguistic values.

The input values are crisp numbers that are converted to fuzzy sets by the fuzzifier. During this process the input values are compared with the membership functions to determine the membership values, indicating the degree of belonging to a linguistic set. The membership functions can have different shapes such as triangle, trapezoidal, Gaussian, Sigmoidal, S-shaped, Z-shaped membership functions.

Knowledge base and the decision-making unit are the main parts of the fuzzy inference system. The knowledge base contains two parts, namely rule base and database. A rule base consists of several "IF-THEN" rules while the database defines the membership functions and includes the fuzzy set. The decision-making unit applies the reasoning operations on the appropriate fuzzy rules and input data. The fuzzy reasoning process involves the following operations: (1) determination of the matching degree between the input data and the fuzzy sets, (2) Calculation of the fire strength

and (3) acquisition of the outputs based on the calculated fire strength [45]. The defuzzifier converts the fuzzy set to a crisp number which is the final result [46]. The commonly used defuzzification methods are: centroid, center of sums, mean of maxima and left-right maxima.

We have used the Fuzzy Logic Toolbox of the MATLAB 2009a in order to built a Mamdani Type Fuzzy Inference System and to classify the nodules as malignant or benign.

The dataset which we used includes 154 chest radiographs with benign and malignant nodules. We divided the dataset randomly into two groups: training and testing set. There are 110 nodules in the training data set which is 70% of all while there are 44 nodules in the testing data set.

We build a Mamdani Type Fuzzy Inference System. The input nodes of the system are the sets of the features: area, perimeter, circularity (irregularity index), equivalent diameter, convex area, solidity, entropy, mean, standard deviation and variance extracted from the benign and malignant nodule regions as explained in Feature Extraction section. Each of the features is represented by a set as follows:

$$A = a1, a2, ..., an \qquad (2.19)$$

$$P = p1, p2, ..., pn \qquad (2.20)$$

where A and P represents the area and the perimeter, respectively.

In the fuzzification layer, two Gaussian membership functions are set up for each of the inputs. The reasons of using Gaussian-distributed membership functions are the limited number of data and the distribution of the Gaussian distributed features. The Fuzzy Logic Toolbox of MATLAB needs two parameters for the valid membership function definition: mean and standard deviation values. Therefore, the mean and

standard deviation of each feature from each nodule type are calculated and taken as the Gaussian parameters for the corresponding membership functions. The names of the membership functions remain as the same: mf1 and mf2 for malignant and benign structures respectively. Creation of the membership functions for the output variables is done in the similar manner and the variables are named as malignant and benign.

The Gaussian membership function can be expressed as:

$$f(x) = e^{-\frac{1}{2}(\frac{x-\mu}{\sigma})^2} \tag{2.21}$$

where μ represents the mean value and δ represents the Standard deviation of the features[46].

After obtaining membership functions from the previous fuzzification layer, the rules are generated from each feature as follows:

Rule 1: IF (area is mf1) AND (perimeter is mf1) .....AND (variance is mf1) THEN (nodule is malignant)

Rule 2: IF (area is mf2) AND (perimeter is mf2) .....AND (variance is mf2) THEN (nodule is benign)

In our method, the fuzzy operator AND was chosen as minimum that means the minimum value of the antecedents is taken:

A AND B = min A, B

where A and B are antecedents

The fuzzy reasoning operation was performed based on the max-min fuzzy inference method. Firstly, a firing strength for each output membership function is

calculated. Then a max-min rule operation was applied in order to generate output response values. At the first step of the process the min fuzzy operation is applied to integrate the inputs for each output class. Then at the second step for aggregation the maximum of all classes was combined.

For deffuzification process the centroid deffuzification technique is applied. According to this method, the center of gravity of the final fuzzy space is taken as the result.

The developed fuzzy inference system for classification is shown in Figure 2.25.
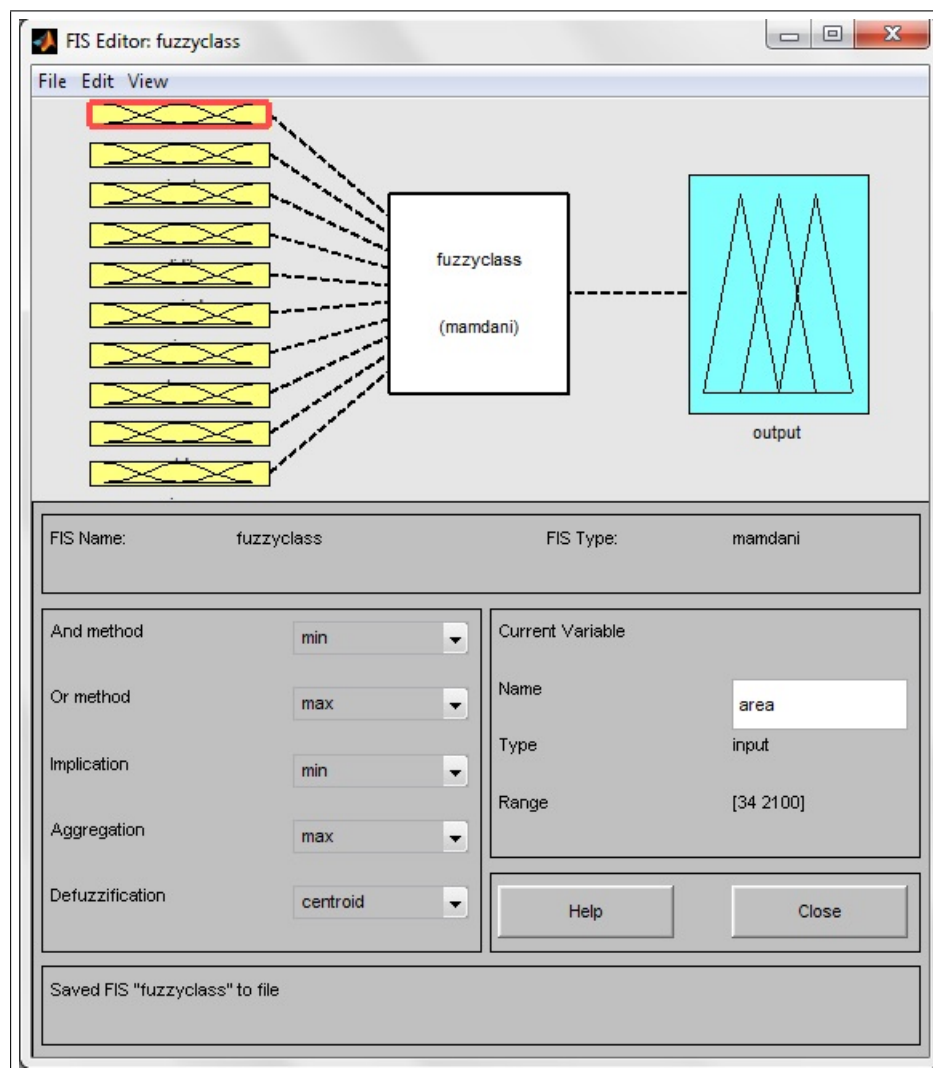

Figure 2.25 General view of lung nodule classification Fuzzy Inference System
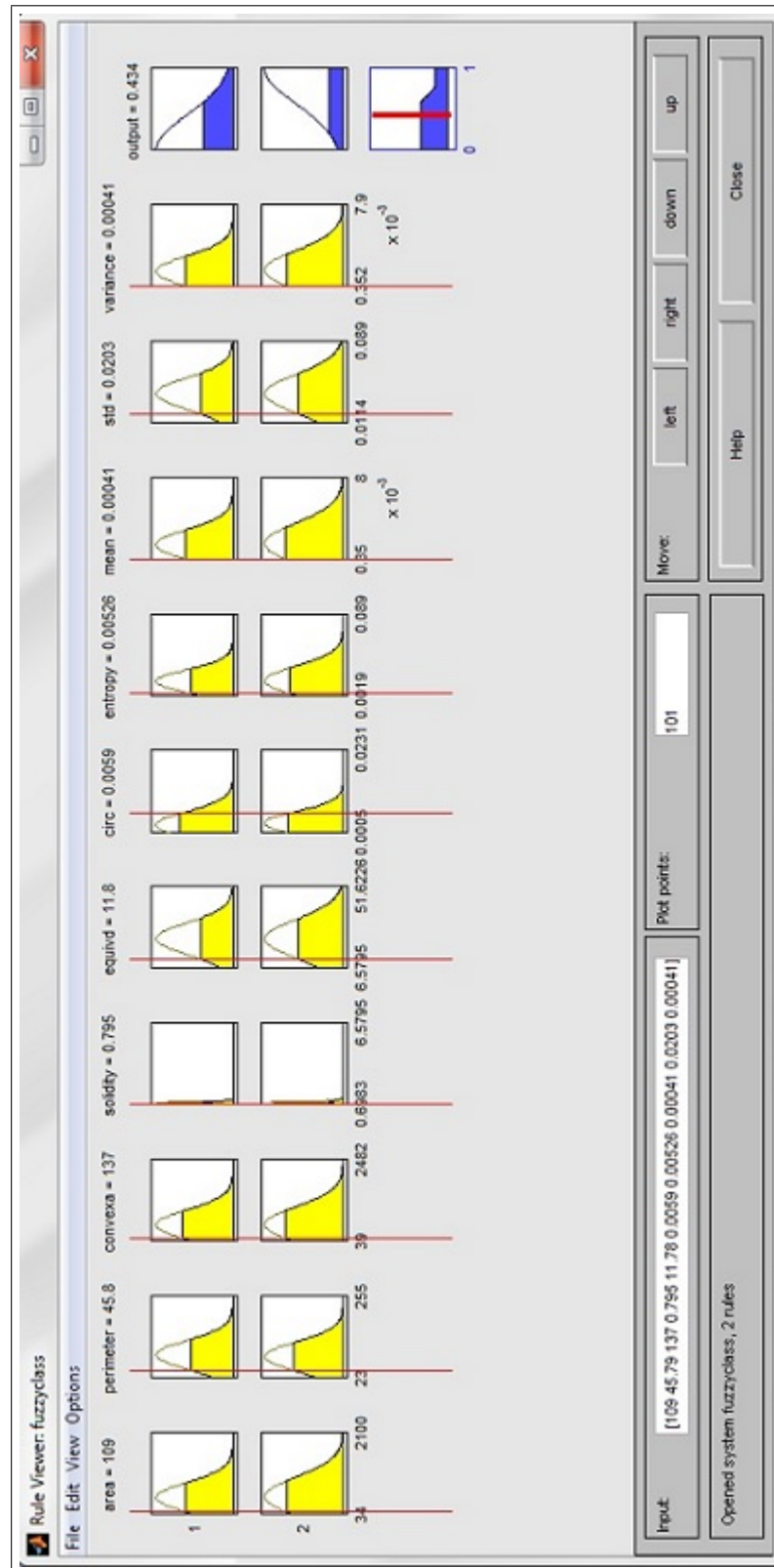
Figure 2.26 Decision-making unit of the Fuzzy Inference System

3. RESULTS & DISCUSSION

In this study, we have used two classification methods namely k nearest neighbor classification and fuzzy classification to characterize the lung nodules as malignant or benign. We have evaluated the performance of these methods in terms of their accuracy. Accuracy is the ratio of the correctly classified nodules to the total number of nodules. The accuracy is calculated as in Eq.3.1.

$$Accuracy = (TP + TN)/(TP + TN + FP + FN) * 100\% \tag{3.1}$$

The confidence interval for the accuracy values were determined for $\pm 95\%$.

We have used 100 malignant and 54 benign nodules to evaluate the system we proposed. 14 features from each nodule were determined as previously mentioned in section 2.6. When we have eliminated the textural features which are contrast, correlation, energy and homogeneity, the results, in terms accuracy remained as the same. Thus, we used 10 features (area, perimeter, convex area, solidity, equivalent diameter, circularity, entropy, mean, standard deviation and variance) for each classification method.

3.1   Results of k-NN Classification

In k-NN classification we used leave-one-out method while testing the system. This method leads us to use all of the nodules to classify the one that we want to classify. We have tested the k-NN classification system for several k values to optimize the accuracy. The results are shown in Table 3.1.

In this case, TP (true positive) represents the correctly classified malignant nodules, FP (false positive) represents the nodules labeled as malignant while they are

Table 3.1
Results of k-NN classification method.

k value	TP	FP	TN	FN	Accuracy (%)
5	79	38	16	21	61.68
15	90	41	13	10	66.80
25	89	40	14	11	66.80
30	90	38	16	10	68.80
35	88	41	13	12	65.50
40	92	52	2	8	61.00
60	100	54	0	0	64.93

benign, TN (true negative) represents the correctly classified benign nodules and FN (false negative) represents the nodules labeled benign while they are actually malignant.

As shown in the Table 3.1 above, the higher accuracy was achieved when the k value is 30. At that level the number of correctly classified malignant nodules is 90 and the number of correctly classified benign nodules is 16. Our initial results indicate that the higher accuracy is 68.8%±7.3 for k-NN classification, which means that 106 nodules out of 154 were classified correctly.

3.2   Results of Fuzzy Classification

We divided the data set as training set and testing set for fuzzy classification. The training set consists of randomly chosen 110 nodules that are approximately 70% of all nodules, while there are 44 nodules in the training set.

The results of this system are shown in Table 3.2.

Table 3.2
Results of Fuzzy Classification Method.

		Prediction	
		malignant	benign
Actual	malignant	15	11
	benign	6	12

There are 27 correctly classified nodules out of 44 nodules in the testing set. Thus, the accuracy for fuzzy classification is 61.3%±14.3.

3.3 Comparison of Classification Techniques

The numbers of classified nodules as true positive, true negative, false positive and false negative according to the classification methods is given in Table 3.3.

According to our initial results, we get a higher accuracy form the k-NN classification method than the fuzzy classification method as shown in Table 3.4. The confidence interval for the accuracy values were determined for ±95%.

Table 3.3
Results of performance measures.

# classified nodules	fuzzy classifier	k-nearest neighbor classifier
TP	15	90
TN	12	16
FP	11	38
FN	6	10

Table 3.4
Results in terms of classification accuracy.

Methods	Accuracy (%)
k-NN Classification	68.8 ±7.3
Fuzzy Classification	61.3 ±14.3

3.4   Discussion

While the previous studies on lung nodule characterization reveal that the developed systems increase the performance of the radiologists, there are no commercially available computerized systems for clinical usage. This is due to the liability concerns for delaying a biopsy while it is necessary. Therefore, we have studied on this issue in order to contribute to the progress. The studies which aim to differentiate the nodules are more performed on CT images than chest x-ray images, because the characterization of malignant lung nodules from benign lung nodules from chest radiographs is a complicated task. However, chest radiography has an extensive usage in the field of lung cancer imaging.

The most common types of classifiers used are linear discriminant classifiers (LDC) and neural networks (NNs). We have used Fuzzy Rule Based classifier and to compare we applied a k-NN classifier. According to our initial results, the accuracy rate obtained from the k-NN classifier is higher than the accuracy rate of the fuzzy classifier which is 68.8% ±7.3 and 61.3% ±14.3, respectively. However, most of the previous studies where both of the classifiers were used, indicated that the performance of the fuzzy classifiers is more efficient than the k-NN classifiers [47, 22]. Therefore, we were expected a higher result from 68.8% for the fuzzy classification method. When we compare our study with other studies where the fuzzy inference systems were used as classifiers, we can say that the main reason for the lower accuracy can be the number of rules. The performance of the system can be improved by increasing the number of generated rules by experts. On the other hand, both of the classification methods have a high sensitivity rate. That means the methods successfully identify

the malignant nodules. A solution to enhance the determination of the benign nodules can be increasing the number of benign nodules in the database.

Based on literature research, it was observed that most of the studies have the potential to improve the accuracy of the nodule detection and characterization processes. When we compare our study with other studies where the classifiers were evaluated in terms of their accuracy, we can say that our study shows promising results. The classification accuracy of the study which is present by Kaya et al. in [22] is 79.5%. Another study which is reported by Hosseini et al. in [23], reaches the rate 67.2% in terms of classification accuracy. In these studies fuzzy classifiers were used in order to differentiate the malignant and benign nodules. In our study, the classification accuracy is 68.8% according to our initial results.

The nodule segmentation process is the most important step for an accurate classification since the features of the nodules is determined according to the segmented nodule areas. As mentioned before in section 2.4.2, for nodule segmentation the multiple delineation option was evaluated with Dr. Hıdır Kaygusuz from Dr. Abdurrahman Yurtaslan Ankara Oncology Training and Research Hospital. According to our initial results the number of correctly segmented nodule rate was increased by 16.7%. The results were found promising for segmentation process especially. The system was also found beneficial especially for teleradiology.

4. CONCLUSION & FUTURE WORK

4.1 Summary of the Study

The primary objective of this study is to develop a semi-automatic computer aided diagnosis system to classify the nodules as malignant or benign to help radiologist diagnose the lung cancer and to prevent the unnecessary biopsies. In this study, we developed a semi-automatic computer aided diagnosis system that mainly consists of five steps: pre-processing, nodule detection, nodule segmentation, feature extraction and nodule classification. In pre-processing step, we aimed to improve the quality of the image by enhancing the contrast of the image and by reducing the noise on the image. This step worked successfully and increased the detection and segmentation rate of the nodules. In the second step, we used template-matching techniques to detect the nodules automatically. The rate of the detected nodules automatically with template matching is 59.7%. This process did not work for all of the elements of the database. In this situation, the detection of the nodules were done by the radiologists manually. The third step is the segmentation. In this part firstly, we matched the histograms of all images according to a reference value which we obtained from an image experimentally and set the window and level values. Secondly, to improve the boundaries of the nodule areas fuzzy minimization was applied. After that, the nodules were segmented with active contours. For our database the process worked for 78 images automatically. We designed an alternative manual system in order to continue the process when the automatic segmentation did not work. In this case, the radiologists segmented the nodules manually from a screen which contains four version of the same chest x-ray image. These four versions are: the original lung image, the image after contrast enhancement and filtering, a pseudo-colored image and the image after applying fuzzy minimization. The manual segmentation rate was improved by using this divided screen. The segmentation rate increased at a rate of 16.7%. From the segmented nodule areas 14 features namely area, perimeter, convex area, solidity, equivalent diameter, circularity, entropy, mean, standard deviation, variance,contrast, correlation, energy

and homogeneity were extracted to use as the inputs of classification methods. Lastly, two classification techniques were used for characterization of tumors namely k-NN classification and fuzzy classification. We evaluated these methods in terms of accuracy. Our initial results indicate that the k-NN classifier has a higher accuracy. To sum up, the initial results obtained show that this methodology has the potential to assist radiologists as a second opinion tool in the classification of benign and malignant lung nodules.

4.2 Future Work

The following items are suggestions for further studies on this system to improve the system performance.

•The negative effects of bone shadows on nodule segmentation can be prevented by applying bone subtraction techniques. This will also provide higher characterization accuracy.

•Multiple image delineation step can be improved by adding the real time option which allows the user to examine the images simultaneously. This issue was discussed with a radiologist from Dr. Abdurrahman Yurtaslan Ankara Oncology Training and Research Hospital. He finds the idea beneficial especially for PAC systems.

•A fully automatic CAD system can be developed by improving the detection and segmentation parts of this system to obtain a faster process.

•Moreover, further development of this CAD system can be done by further testing with larger sample sizes.

•The effects of the selected features on the classification of nodules can be analyzed in more detail.

●Another improvement can be done on fuzzy classification method by applying more rules with the help of radiologists to increase the accuracy.

●The performance of the fuzzy classifier can be tested with different types of fuzzy inference methods.

REFERENCES

1. Ferlay, J., I. Soerjomataram, R. Dikshit, S. Eser, C. Mathers, M. Rebelo, D. M. Parkin, D. Forman, and F. Bray, "Cancer incidence and mortality worldwide: sources, methods and major patterns in globocan 2012," *International Journal of Cancer*, Vol. 136, no. 5, pp. E359–E386, 2015.

2. Van Ginneken, B., B. M. ter Haar Romeny, M. Viergever, *et al.*, "Computer-aided diagnosis in chest radiography: a survey," *Medical Imaging, IEEE Transactions on*, Vol. 20, no. 12, pp. 1228–1241, 2001.

3. Shiraishi, J., Q. Li, K. Suzuki, R. Engelmann, and K. Doi, "Computer-aided diagnostic scheme for the detection of lung nodules on chest radiographs: localized search method based on anatomical classification," *Medical Physics*, Vol. 33, no. 7, pp. 2642–2653, 2006.

4. Katsuragawa, S., and K. Doi, "Computer-aided diagnosis in chest radiography," *Computerized Medical Imaging and Graphics*, Vol. 31, no. 4, pp. 212–223, 2007.

5. Giger, M. L., H.-P. Chan, and J. Boone, "Anniversary paper: History and status of cad and quantitative image analysis: the role of medical physics and aapm," *Medical physics*, Vol. 35, no. 12, pp. 5799–5820, 2008.

6. Bomma, P., *Comupter-aided diagnosis tool for the detection of cancerous nodules in x-ray images*. PhD thesis, Louisiana State University and Agricultural and Mechanical College, 2005.

7. Siegel, R., J. Ma, Z. Zou, and A. Jemal, "Cancer statistics, 2014," *CA: a cancer journal for clinicians*, Vol. 64, no. 1, pp. 9–29, 2014.

8. Röntgen, W. K., *Ueber eine neue Art von Strahlen:(Sitzungsberichte der phys.-med. Gesellschaft Würzburg)*, Springer, 1949.

9. Chen, S., K. Suzuki, and H. MacMahon, "Development and evaluation of a computer-aided diagnostic scheme for lung nodule detection in chest radiographs by means of two-stage nodule enhancement with support vector classification," *Medical physics*, Vol. 38, no. 4, pp. 1844–1858, 2011.

10. Samei, E., M. J. Flynn, E. Peterson, and W. R. Eyler, "Subtle lung nodules: Influence of local anatomic variations on detection 1," *Radiology*, Vol. 228, no. 1, pp. 76–84, 2003.

11. Delrue, L., R. Gosselin, B. Ilsen, A. Van Landeghem, J. de Mey, and P. Duyck, "Difficulties in the interpretation of chest radiography," in *Comparative Interpretation of CT and Standard Radiography of the Chest*, pp. 27–49, Springer, 2011.

12. Doi, K., "Computer-aided diagnosis in medical imaging: historical review, current status and future potential," *Computerized medical imaging and graphics*, Vol. 31, no. 4, pp. 198–211, 2007.

13. Shiraishi, J., Q. Li, D. Appelbaum, and K. Doi, "Computer-aided diagnosis and artificial intelligence in clinical imaging," in *Seminars in nuclear medicine*, Vol. 41, pp. 449–462, Elsevier, 2011.

14. Doi, K., "Overview on research and development of computer-aided diagnostic schemes," in *Seminars in Ultrasound, CT and MRI*, Vol. 25, pp. 404–410, Elsevier, 2004.

15. Firmino, M., A. H. Morais, R. M. Mendoça, M. Dantas, H. Hekis, and R. Valentim, "Computer-aided detection system for lung cancer in computed tomography scans: Review and future prospects," *Biomed Eng Online*, Vol. 13, pp. 1–16, 2014.

16. Doi, K., "Current status and future potential of computer-aided diagnosis in medical imaging," *The British Journal of Radiology*, 2014.

17. PATIL, D. S., and M. Kuchanur, "Lung cancer classification using image processing," *International Journal of Engineering and Innovative Technology (IJEIT) Volume*, Vol. 2, 2012.

18. Al Gindi, A. M., T. A. Attiatalla, and M. M. Sami, "A comparative study for comparing two feature extraction methods and two classifiers in classification of earlystage lung cancer diagnosis of chest x-ray images," *J Am Sci*, Vol. 10, pp. 13–22, 2014.

19. Suzuki, K., F. Li, S. Sone, *et al.*, "Computer-aided diagnostic scheme for distinction between benign and malignant nodules in thoracic low-dose ct by use of massive training artificial neural network," *Medical Imaging, IEEE Transactions on*, Vol. 24, no. 9, pp. 1138–1150, 2005.

20. Shiraishi, J., H. Abe, R. Engelmann, M. Aoyama, H. MacMahon, and K. Doi, "Computer-aided diagnosis to distinguish benign from malignant solitary pulmonary nodules on radiographs: Roc analysis of radiologistsâ performanceâinitial experience 1," *Radiology*, Vol. 227, no. 2, pp. 469–474, 2003.

21. Aoyama, M., Q. Li, S. Katsuragawa, H. MacMahon, and K. Doi, "Automated computerized scheme for distinction between benign and malignant solitary pulmonary nodules on chest images," *Medical Physics*, Vol. 29, no. 5, pp. 701–708, 2002.

22. Kaya, A., and A. B. Can, "efis: A fuzzy inference method for predicting malignancy of small pulmonary nodules," in *Image Analysis and Recognition*, pp. 255–262, Springer, 2014.

23. Hosseini, R., J. Dehmeshki, S. Barman, M. Mazinani, A.-M. Jouannic, and S. Qanadli, "A fuzzy logic system for classification of the lung nodule in digital images in computer aided detection," in *Digital Society, 2010. ICDS'10. Fourth International Conference on*, pp. 255–259, IEEE, 2010.

24. Shiraishi, J., S. Katsuragawa, J. Ikezoe, T. Matsumoto, T. Kobayashi, K.-i. Komatsu, M. Matsui, H. Fujita, Y. Kodera, and K. Doi, "Development of a digital image database for chest radiographs with and without a lung nodule: receiver operating characteristic analysis of radiologists' detection of pulmonary nodules," *American Journal of Roentgenology*, Vol. 174, no. 1, pp. 71–74, 2000.

25. Nixon, M., *Feature extraction & image processing*, Academic Press, 2nd ed., 2008.

26. Damodhar, J., and D. Sathyanarayana, "Implementation of contrast stretching algorithm on lung cancer effected images for analysis," in *International conference on Advanced Computing, Communication and Networks'11*, pp. 964–969, 2011.

27. Tarambale, M. r., and N. s. Lingayat, "Soft tool developement for characterization of lung nodule from chest x-ray image," Vol. 2, no. 1, pp. 7–12, 2012.

28. Sherrier, R. H., and G. Johnson, "Regionally adaptive histogram equalization of the chest," *Medical Imaging, IEEE Transactions on*, Vol. 6, no. 1, pp. 1–7, 1987.

29. Sarage, G., and S. Jambhorkar, "Enhancement of chest x-ray images using filtering techniques," *Int J Adv Res Comput Sci Softw Eng*, Vol. 2, pp. 308–12, 2012.

30. Zhou, J., *Computer Aided Diagnosis of Lung Ground Glass Opacity Nodules and Large Lung Cancers in CT.*, ProQuest, 2008.

31. Lee, Y., T. Hara, H. Fujita, S. Itoh, and T. Ishigaki, "Automated detection of pulmonary nodules in helical ct images based on an improved template-matching technique," *Medical Imaging, IEEE Transactions on*, Vol. 20, no. 7, pp. 595–604, 2001.

32. Li, Q., S. Katsuragawa, and K. Doi, "Computer-aided diagnostic scheme for lung nodule detection in digital chest radiographs by use of a multiple-template matching technique," *Medical Physics*, Vol. 28, no. 10, pp. 2070–2076, 2001.

33. El-Baz, A., G. M. Beache, G. Gimel'farb, K. Suzuki, K. Okada, A. Elnakib, A. Soliman, and B. Abdollahi, "Computer-aided diagnosis systems for lung cancer: challenges and methodologies," *International journal of biomedical imaging*, Vol. 2013, 2013.

34. Tizhoosh, H. R., "Fuzzy image enhancement: an overview," in *Fuzzy techniques in image processing*, pp. 137–171, Springer, 2000.

35. Pal, S. K., R. King, *et al.*, "Image enhancement using smoothing with fuzzy sets," *IEEE TRANS. SYS., MAN, AND CYBER.*, Vol. 11, no. 7, pp. 494–500, 1981.

36. Patil, S., and V. Udupi, "Geometrical and texture features estimation of lung cancer and tb images using chest x-ray database," *International Journal of Biomedical Engineering and Technology*, Vol. 6, no. 1, pp. 58–75, 2011.

37. Lingayat, N. S., and M. R. Tarambale, "A computer based feature extraction of lung nodule in chest x-ray image," *International Journal of Bioscience, Biochemistry and Bioinformatics*, Vol. 3, no. 6, pp. 624–629, 2013.

38. Lee, T. K., D. I. McLean, and M. S. Atkins, "Irregularity index: a new border irregularity measure for cutaneous melanocytic lesions," *Medical image analysis*, Vol. 7, no. 1, pp. 47–64, 2003.

39. Gonzalez, R. C., R. E. Woods, and S. L. Eddins, *Digital image processing using MATLAB*, Pearson Education India, 2004.

40. Choras, R. S., "Image feature extraction techniques and their applications for cbir and biometrics systems," *International journal of biology and biomedical engineering*, Vol. 1, no. 1, pp. 6–16, 2007.

41. Mangai, J. A., S. Wagle, and V. S. Kumar, "An improved k nearest neighbor classifier using interestingness measures for medical image mining," *Engineering and Technology International Journal of Medical, Health*, Vol. 7, no. 9, pp. 236–240, 2013.

42. Perez, M., and T. Marwala, "The fuzzy gene filter: A classifier performance assesment," *arXiv preprint arXiv:1108.4545*, 2011.

43. Riza, L. S., C. Bergmeir, F. Herrera, and J. Benitez, "frbs: Fuzzy rule-based systems for classification and regression in r," *Journal of Statistical Software*, Vol. 65, no. 6, pp. 1–30, 2015.

44. Samuel, C. C., V. Saravanan, and M. V. Devi, "Lung nodule diagnosis from ct images using fuzzy logic," in *Conference on Computational Intelligence and Multimedia Applications, 2007. International Conference on*, Vol. 3, pp. 159–163, IEEE, 2007.

45. Pappis, C. P., and C. I. Siettos, "Fuzzy reasoning," in *Search Methodologies*, pp. 437–474, Springer, 2005.

46. Sivanandam, S., S. Sumathi, S. Deepa, *et al.*, *Introduction to fuzzy logic using MATLAB*, Vol. 1, Springer, 2007.

47. Mahdi, A., A. Razali, and A. AlWakil, "Comparison of fuzzy diagnosis with k-nearest neighbor and naïve bayes classifiers in disease diagnosis," *BRAIN. Broad Research in Artificial Intelligence and Neuroscience*, Vol. 2, no. 2, pp. 58–66, 2011.